Yunpeng Ye[1]
Min Liu[1,†]
Jeff L.-K. Kao[2]
Garland R. Marshall[1]
[1] *Department of Biochemistry and Molecular Biophysics, Washington University, St. Louis, MO 63110*

[2] *Department of Chemistry, Washington University, St. Louis, MO 63110*

Received 25 February 2003; accepted 6 May 2003

Peptide-Bond Modification for Metal Coordination: Peptides Containing Two Hydroxamate Groups*

Abstract: *Peptide-bond modification via* N*-hydroxylation has been explored as a strategy for metal coordination to induce conformational rigidity and orient side chains for specific molecular recognition.* N*-Hydroxyamides were prepared by reacting N-benzyloxyamino acid esters or amides with Fmoc–AA–Cl/AgCN (Fmoc: 9-fluorenylmethoxycarbonyl; AA: amino acid) in toluene or Fmoc–AA/HATU/DIEA in DMF (HATU: O-(7-azabenzotriazol-lyl)-1,1,3,3-tetramethyluronium hexafluorophosphate; DIEA:* N,N*-diisopropylethylamine; DMF:* N,N*-dimethylformamide), followed by deblocking of benzyl protecting groups. Novel linear and cyclic* N,N′*-dihydroxypeptides were efficiently assembled using Fmoc chemistry in solution and/or on a solid support. As screened by electrospray ionization–mass spectroscopy (ESI-MS), high iron-binding selectivity and affinity were attainable. Compounds having a spacer of two α-amino acids between the amino acids bearing the two hydroxamates, i.e., a spacer of 8 atoms, generated 1:1 iron complex species in the gas phase. Moreover, high performance liquid chromatography (HPLC), uv/vis, and* ^{1}*H-NMR analyses provided direct evidence for complex formations in solution. Significantly, the representative compound cyclo(Leu–Ψ[CON(OH)]–Phe–Ala–Pro)*$_2$ *(**P8**) may serve as a robust metal-binding scaffold in construction of a metal-binding library for versatile metal-mediated molecular recognition.*
 Biopolymers (Pept Sci) 71: 489–515, 2003

Keywords: *peptide-bond modification; metal coordination; conformational rigidity; molecular recognition; N-hydroxyamide; hydroxamate*

INTRODUCTION

Metals play essential roles in biological systems both structural and functional. Iron exists at the active center of proteins responsible for oxygen and electron transport. Functional roles of metals are found in such diverse metalloenzymes as oxidases, hydrogenases, reductases, dehydrogenases, deoxygenases, and dehy-

Correspondence to: Garland R. Marshall; email: garland@ibc.wusl.edu

* Part of this work was presented at the 17th American Peptide Symposium, San Diego, California, June 9–14, 2001

† *Present address:* Pfizer, Inc., 700 Chesterfield Parkway North, Chesterfield, MO 63198

Contract grant sponsor: National Institutes of Health
Contract grant number: GM 536305

Biopolymers (Peptide Science), Vol. 71, 489–515 (2003)

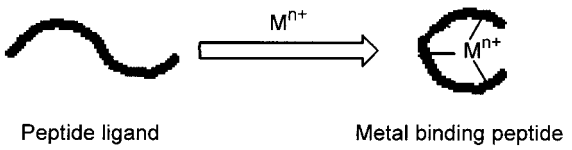

FIGURE 1 Schematic representation of preorganization and conformational constraint for peptides via metal coordination.

drases.[1] Zinc organizes the conformation required for molecular recognition in zinc-finger proteins, originally isolated as transcription factors, but now recognized as having diverse functions in biology.[2] Metal-binding compounds have received great attentions for their potentials in conformational control, biomimetic design, elucidation of metal-mediated catalytic mechanism, and chelation therapy, as novel enzyme inhibitors, and in the development of metallo-drugs, etc.[1] We[3–7] and others[8–12] have utilized metal coordination as a strategy for preorganizing peptide structures for molecular recognition by enzymes and receptors. Others have used metal coordination as a means of stabilizing secondary structures[13–18] and quaternary structures such as coiled coils[19] and helix bundles[20] as well as controlling the allosteric states of receptors.[21,22] Coordination of different metals allows subtle variation of the conformation of ligands with the same molecular template[23] that should assist elucidating the receptor-bound conformation and optimizing the complementarity between peptide ligand and enzyme/receptor (Figure 1).

Most reports of metal-binding peptides and peptidomimetics focus on metal–peptide complexes utilizing peptide side chains, the amino, imidazole, carboxylate, sulfhydry, indole, phenol groups, etc., as metal-binding sites. As side chains of peptides often play very important roles in molecular recognition at biological receptors, we have focused on modifying peptide bonds to build metal-binding sites within the backbone.[3–7] This strategy leaves the side chains free to interact with receptors while the conformation of the backbone is preorganized via metal coordination. As combinatorial approaches have proved valuable for the discovery of molecules with novel structures having interesting biological activities,[24–29] we sought to develop metal-binding scaffolds that would be useful in efficient construction of a metal-binding library. Metal coordination is expected to not only preorganize the complex's conformation for molecular recognition, but the use of different metals will also enhance structural diversity by subtle conformational effects on the template that orients the side chains.

We envision that an ideal metal-binding scaffold should be endowed with the following features: (1) exhibits high metal-binding affinity and selectivity generating a limited number of stable structures; (2) coordinates a single metal ion specifically within the ligand architecture; (3) allows for the generation of high structural diversity and similarity via an efficient combinatorial approach; and (4) possesses significantly diverse bioactivities where the structure–function relationships can be explored by metal coordination. As peptides are common chemical messengers in biological systems, we sought minimal structural perturbation that would confer metal-binding properties on the peptide backbone. It is well known that a hydroxamate group is a very powerful bidentate ligand for metal coordination. For example, the naturally occurring trihydroxamate-containing siderophores such as desferrioxamine (DFO) bind and transport ferric ions essential for growth and proliferation of microorganisms.[30] The conformation, metal-binding properties, and interesting biological activities of *N*-hydroxypeptides have received attention. Peptidyl hydroxamic acids have been developed as potent inhibitors of several metalloproteases[31–34] including matrix metalloproteinases.[35–37] Hin et al.[38] reported that *N*-hydroxylation of a single amide bond in the T-cell epitope SIINFEKL[39] by replacement of Asn with *N*-hydroxyglycine renders a T-cell receptor agonist into an antagonist and enhances enzymatic stability. Recently, hydroxamate-containing peptidomimetics show significant inhibition of HIV protease in vitro.[40] The metal-binding properties and potential biological activities of peptides containing multiple *N*-hydroxyamides led to exploration of *N*-hydroxyamide-containing peptides as metal-binding scaffolds.

Earlier efforts to design and synthesize tri-*N*-hydroxamide-containing peptides by mimicking the siderophore, DFO, were reported by the Akiyama group.[41,42] More recent studies[43,44] by Hara et al. have focused on iron complexation by oligomers of Ala–Ala–Ψ[CO–NOH]–β-Ala. In contrast, we initially focused on *N,N′*-dihydroxypeptides. Dihydroxamic acids, such as the siderophore rhodotorulic acid and its analogs have been reported to form 1:1 complexes with iron(III) at low pH.[45–47] While a cyclic *N,N′*-dihydroxy dipeptide has been reported,[48] to the best of our knowledge, metal-binding properties of *N,N′*-dihydroxypeptides have not been characterized. Compared to hexadentate *N,N′,N″*-trihydroxypeptides, tetradentate *N,N′*-dihydroxypeptides possess only two bidentate metal-binding motifs. Nevertheless, in order to efficiently construct metal-binding libraries containing multiple *N*-hydroxamide groups, a close scrutiny of *N,N′*-dihyroxypeptides and their metal-binding properties was the initial goal. First, it would provide understanding of the structure vs metal-binding properties; second, it should help in the ra-

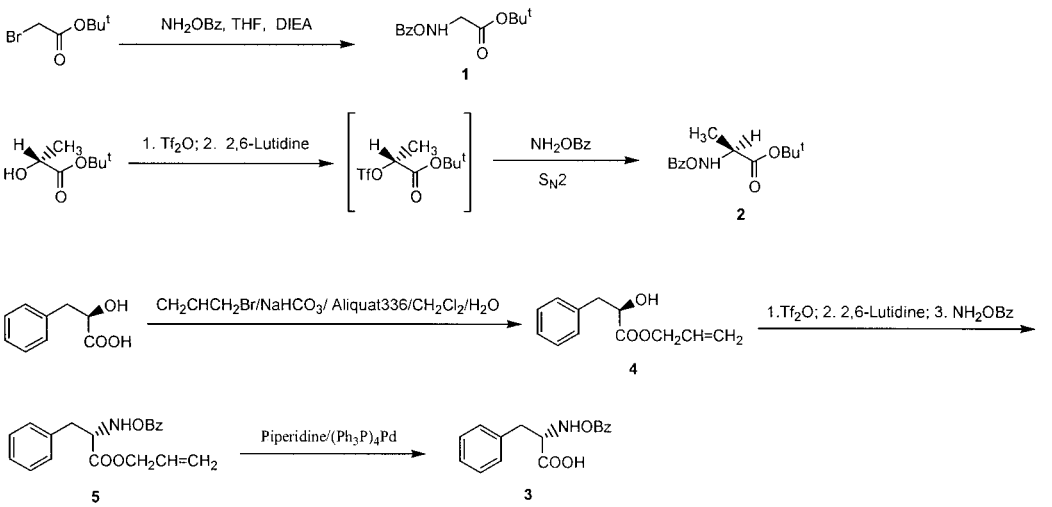

SCHEME 1 Synthesis of *N*-benzyloxy-glycine *t*-butyl ester (**1**), *N*-benzyloxy-alanine *t*-butyl ester (**2**), and *N*-benzyloxyphenylalanine (**3**) as building blocks. THF: tetrahydrofurane; DIEA: *N,N*-diisopropylethylamine.

tional design of improved *N,N′,N″*-trihydroxypeptides; third, a robust and compact metal-binding scaffold based on *N,N′*-dihydroxypeptides would allow the rational incorporation of additional versatile metal-binding sites (in side chains, for example) for further molecular diversity.

The aims of this study were as follows: (a) to develop efficient syntheses of *N,N′*-dihydroxypeptides; (b) to establish rapid methods for screening their metal-binding properties; (c) to elucidate the structure vs metal-binding relationship for further molecular design and other potential applications; and finally, to provide a metal-binding scaffold for construction of a two-dimensional combinatorial library where ligand structure would comprise one dimension, and different bound metals would compromise the second dimension.

SYNTHESIS

Initially, novel dihydroxamate-containing pseudo-oligopeptides that featured one hydroxamate group at the C-terminus and the other close to the N-terminus using an oligopeptide sequence as linker were targeted. The synthetic route to such *N,N′*-dihydroxy-oligopeptides should allow facile synthesis in solution phase and/or on a solid support.

$$X_{AAl}\text{–}\Psi[CON(OH)]\text{–}X_{AAl}\text{—}[Spacer]\text{—}X_{AAn}\text{–}\Psi[CONH(OH)]$$

C-terminal hydroxamic acids [CONH(OH)] were readily accessible from hydroxylamine derivatives in solution or on a solid support[49,50] while the internal hydroxamic acid [—CON(OH)—] could be synthesized by acylation of protected *N*-hydroxyamino acid derivatives prepared by a variety of procedures.[51–54] Three *O*-benzyl protecting *N*-hydroxy-α-amino acids derivatives were used as building blocks, i.e., *N*-benzyloxy-glycine *tert*-butyl ester **1,** *N*-benzyloxy-alanine *tert*-butyl ester **2,** and *N*-benzyloxy-phenylalanine **3** for application to Fmoc-based peptide synthesis (Fmoc: 9-fluorenyl-methoxycarbonyl). Transformation of primary amines into hydroxyamines via direct oxidation has proven difficult due to further oxidation to form nitroso and nitro compounds, especially for preparation of optically active *N*-hydroxyamino acids. Versatile methods for indirect preparation of *N*-hydroxyamino acid derivatives have been reported.[55–63] Among them, Feenstra et al.[56] reported that protected *N*-hydroxyamino acids of high optical purities were prepared from their corresponding α-hydroxy ester via triflates in high yields. As shown in Scheme 1, **1** was readily prepared from α-bromoacetic acid *tert*-butyl ester and *O*-benzylhydroxylamine. According to Feenstra et al.,[56] **2** was prepared from commercially available D-(-)-lactic acid *t*-butyl ester via its triflate intermediate, followed by the attack of *O*-benzyl-hydroxylamine in situ. The overall yield of **2** from the lactic acid ester was 65%. The synthesis of **3** was similarly carried out starting from commercially available D-3-phenyllactic acid that was first converted to the corresponding allyl ester **4.**[64] The resulting *N*-benzyloxyphenylalanine allyl ester **5** was deblocked with piperidine/$Pd(PPh_3)_4$ to afford **3** with an overall yield of 55%. It is noteworthy that the attack of benzyloxyamine via an S_N2 mechanism led to inversion of configuration.

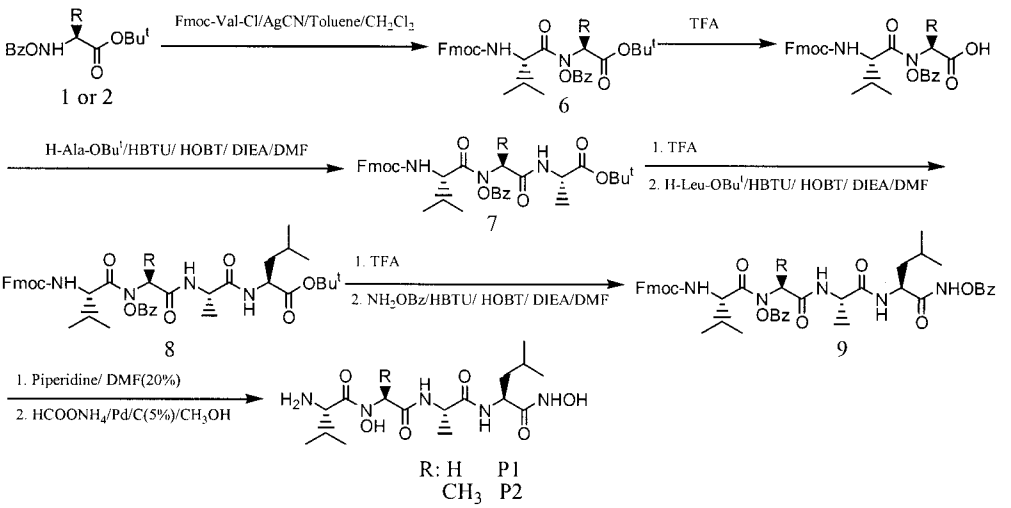

SCHEME 2 Incorporation of *N*-benzyloxy-glycine *tert*-butyl ester and *N*-benzyloxy-alanine *tert*-butyl ester into peptides. HBTU: *O*-benzotriazole-*N,N,N′,N′*-tetramethyluronium hexafluorophosphate; DMF: *N,N*-dimethylformamide; HOBT: 1-hydroxybenzotriazole.

Compared to the amino groups of usual amino acid building blocks, the amino groups of *N*-benzyloxy-amino acid derivatives have poor basicity and nucleophilicity due to the steric and electronic effects of the *N*-benzyloxy group.[55] Powerful acylation methods, such as acid chloride, mixed anhydride, and O-(7-azabenzotriazol-lyl)-1,1,3,3-tetramethyluronium hexafluorophosphate (HATU), were required for efficient syntheses of *N*-hydroxypeptides. Compared to the amino acid anhydride and HATU methods, the acid chloride method was attractive due to its facile preparation from the corresponding Fmoc-amino acid and oxalyl chloride in DCM. Importantly, acylation with Fmoc–AA chlorides (AA: amino acid) reportedly occurs without significant racemization.[65] In addition, for solution synthesis, product purification was facilitated without the side products derived from other coupling agents. Perlow et al. successfully used Fmoc–L-isoleucine acid chloride in the acylation of a sterically hindered *N*-Cbz-piperazic acid N-terminus, and the acylation efficiency was further improved by the combination with AgCN in toluene.[66] This powerful acylation method, therefore, was applied to the incorporation of *N*-benzyloxyamino acids into peptides in solution. Wang and Phanstiel[51] have also successfully acylated *N*-(benzoyloxy)amino acid derivatives with Fmoc–amino acid chlorides without racemization. Braslau et al.[67] have utilized a rearrangement of *O*-acyl hydroxamic substrates prepared by coupling Fmoc-amino acid chlorides to *N*-protected hydroxylamine esters to generate di- and tripeptide hydroxamic acids.

As summarized in Scheme 2, the reaction of *N*-benzyloxyglycine *t*-butyl with Fmoc–Val–Cl in the presence of AgCN in toluene afforded dipeptide **6** (85%). Cleavage of the *t*-butyl group of **4** with TFA provided the corresponding acid that was coupled with alanine *t*-butyl ester to give tripeptide **7**. A tetrapeptide **8** was obtained from **7** similarly via cleavage with TFA and then coupling with leucine *tert*-butyl ester. Compound **8** was further coupled with *O*-benzylhydroxylamine to give **9.** Following removal of the Fmoc group with 20% piperidine in DMF, the two *O*-Bz protecting groups were removed successfully with ammonium formate in the presence of Pd/C (5%) in CH_3OH[52] to afford the desired pseudopeptide **P1** with one hydroxamate close to the N-terminus and the other one located at the C-terminus. Based on the above Fmoc/*t*-butyl chemistry in solution, **P2** was prepared from **2** similarly.

In contrast, the low nucleophilicity of the *N*-benzyloxyamino group allowed us to link the carboxylate of *N*-benzyloxy-phenylalanine with the free amino group of a normal amino acid or peptide building block using conventional peptide coupling methods without further protecting the *N*-benzyloxyamino group.

As summarized in Scheme 3, **3** was coupled with alanine *tert*-butyl ester smoothly using EDCI and HOBT in DCM to afford dipeptide **10** in high yield. Similarly, **10** was also reacted with Fmoc–Leu–Cl/AgCN in toluene to afford the tripeptide Fmoc–Leu–Ψ[CON(OBz)]–Phe–Ala–OBu^t (**11**) that was further elongated to give the tetrapeptide, Fmoc–Leu–Ψ[CON(OBz)]–Phe–Ala–Pro–OBu^t (**12**).

The pseudo-peptide **12** was deblocked with 20% piperidine/DMF or 50% TFA/DCM (DCM: dichloromethane) to afford two different intermediates **13**

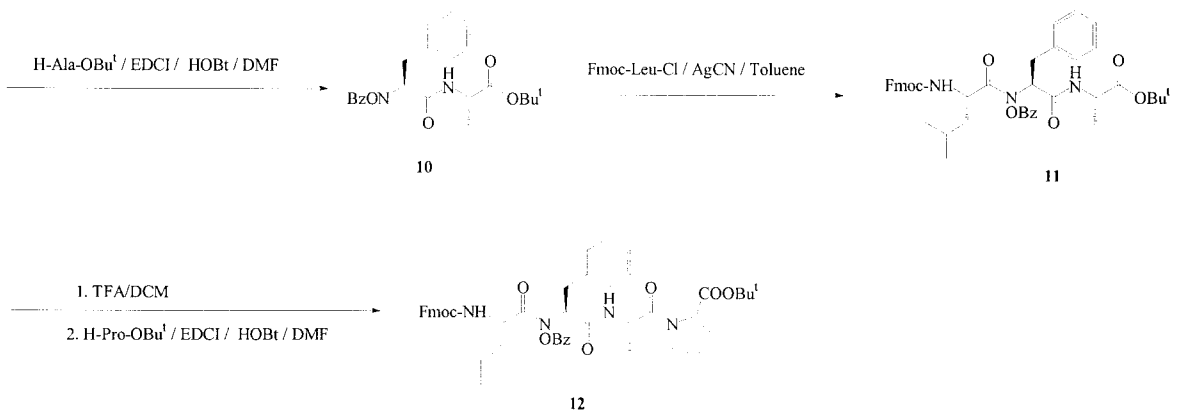

SCHEME 3 Incorporation of benzyloxyphenylalanine into peptides. EDC: 1-(3-dimethylaminopropyl)-3-ethyl-carbodiimide hydrochloride.

and **14** with different free termini that were used as modules to assembly the target compounds via fragment condensation reactions, either in solution or on a solid support. For example, **13** was coupled with **14** in solution to form the dimer **15.** After further deprotecting **15** with piperidine/DMF and TFA/DCM, the resulting linear octapeptide **16** was cyclized in the presence of (benzotriazol-1-yloxy)-tris(pyrrolidino)phosphonium hexafluorophosphate (PyBOP)[68] and DIEA in DMF to afford **17.** Finally, two target compounds, the linear **P7** and its cyclic analog **P8,** were obtained by deprotecting **16** and **17,** respectively. (See Scheme 4.)

The modular approach described above has provided convenient access to a small library of mono-, di-, and tri-hydroxamate-containing pseudo-oligopeptides, making use of *N*-benzyloxyamino acids as building blocks in solution syntheses. Meanwhile, solution methods were adapted to solid phase because of the advantages, i.e., facile workup by filtration, and nearly complete coupling reactions driven via excessive reactants and repeated couplings. As summarized in Scheme 5, solid-phase synthesis started with commercially available *N*-Fmoc-hydroxyamine 2-chlorotrityl resin[50] to introduce the *N*-hydroxamate at the C-terminus. The peptide chain was elongated using

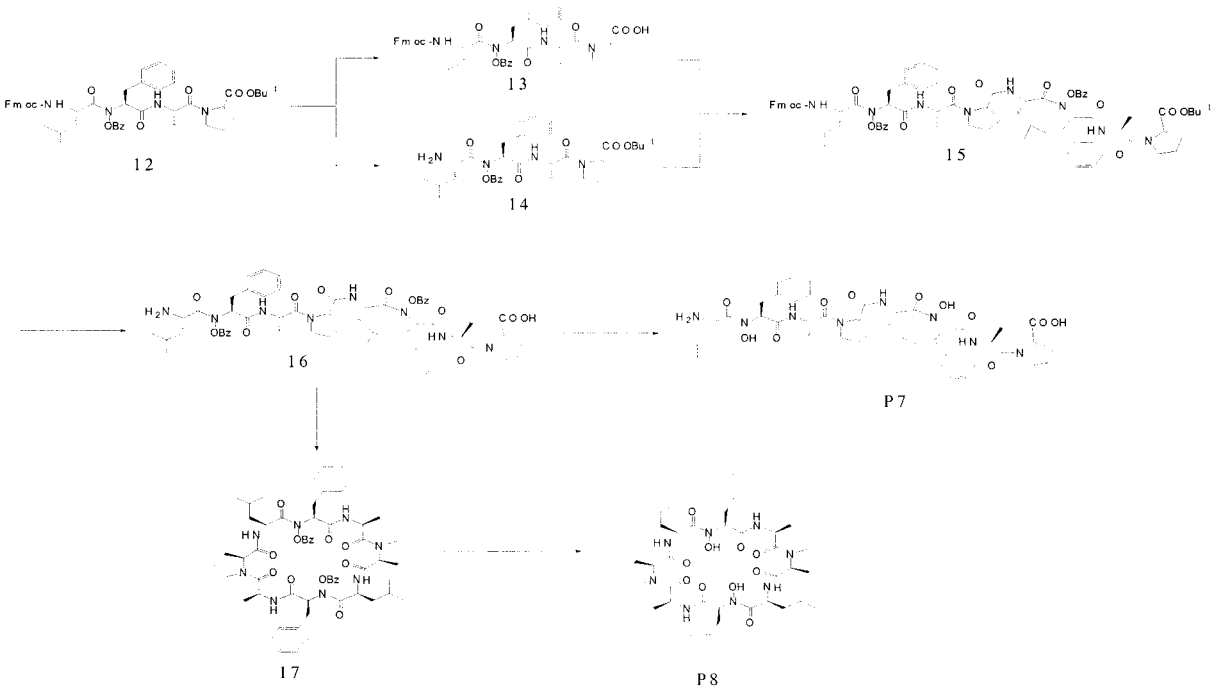

SCHEME 4 Synthesis of linear and cyclic analogs (**P7** and **P8**) of dihydroxamate pseudopeptides using Fmoc–Leu–Ψ[CON(OBz)]–Phe–Ala–Pro–OBu^t (**12**) as a module.

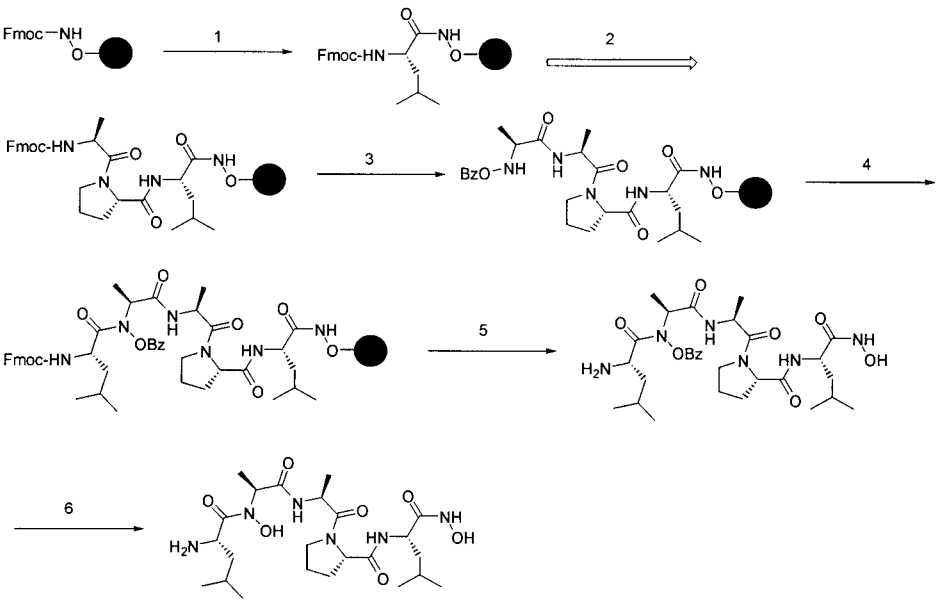

Reagents and conditions: 1. a) Piperidine/DCM(20%), 0.5h; b) Fmoc-Leu/HATU/DIEA, 20h; 2. Chain elongation/Fmoc chemistry; 3. N-BzO-AA/DIC/HOBT, 12h; 4. Fmoc-Leu/HATU/DIEA or Fmoc-Leu-Cl/AgCN/Toluene; 5. a) Piperidine/DMF(20%), 0.5h; b) TFA/DCM(5%), 15 min; 6. $HCOONH_4/Pd/C(5\%)/CH_3OH$.

SCHEME 5 Assembly of the linear dihydroxamate-containing pseudopeptides with one hydroxamic acid at the C-terminus and the other close to the N-terminus on a solid support. DIC: *N,N′*-diisopropylcarbodiimide.

conventional Fmoc chemistry after removal of the Fmoc group and attachment of the first amino acid using HATU/DIEA in DMF. As described in Scheme 5, the *N*-benzyloxyamino acids were similarly incorporated on the solid support using DIC/HOBT without further protecting their *N*-benzyloxyamino groups. Completion of this coupling was conveniently monitored by the ninhydrin test[69] as the benzyloxyamino group was negative to this test. By cleaving an aliquot of the resin and detecting the product by electrospray ionization–mass spectroscopy (ESI-MS), no attachment of additional *N*-benzyloxyamino acid to the desired products were found. In order to form the *N*-benzyloxyamide efficiently on solid phase, HATU that has proven a powerful activating agent in many difficult coupling reactions was used.[39,70] After cleavage with TFA, the isolated products proved that the coupling mediated by HATU were successful.

As showed in Table I, an array of *N,N′*-dihydroxypeptides were designed and synthesized using both solution and solid-phase methods. All the products were purified by semipreparative HPLC, and their purity and identity confirmed by analytical HPLC, ESI-MS, and ^{1}H-NMR. These compounds were designed to probe the effects of structural factors including the spacer between two hydroxamate binding sites, the side chains, and backbone cyclization on metal-binding properties.

Our results show that a library of hydroxamate-containing peptides with structural diversity and similarity can be efficiently constructed by varying the amino acids, the number and positions of *N*-hydroxylation, and the linker between the two hydroxamates in solution or on a solid support. Obviously, the key steps are the couplings with benzyloxyamino groups

Table I The Synthesized *N,N′*-Dihydroxypeptides[a]

Entry	Sequence
P1	H–Val–Ψ[CON(OH)]–Gly–Ala–Leu–NHOH
P2	H–Val–Ψ[CON(OH)]–Ala–Ala–Leu–NHOH
P3	H–Val–Ψ[CON(OH)]–Phe–Ala–Leu–NHOH
P4	H–Val–Ψ[CON(OH)]–Phe–Ala–Pro–Leu–NHOH
P5	H–{Leu–Ψ[CON(OH)]–Phe–Ala}$_2$–OH
P6	Cyclo–{Leu–Ψ[CON(OH)]–Phe–Ala}$_2$
P7	H–{Leu–Ψ[CON(OH)]–Phe–Ala–Pro}$_2$–OH
P8	Cyclo–{Leu–Ψ[CON(OH)]–Phe–Ala–Pro}$_2$
P9	H–Leu–Ψ[CON(OH)]–Phe–Ala–Pro–Leu–NHOH
P10	H–Leu–Ψ[CON(OH)]–Ala–Ala–Pro–Leu–NHOH
P11	H–Leu–Ψ[CON(OH)]–Phe–Ala–Pro–Ala–Leu–NHOH
P12	H–Leu–Ψ[CON(OH)]–Phe–Ala–NHOH

[a] **P1, P2, P3, P4, P9,** and **P12** were synthesized in solution phase as depicted in Scheme 2; **P5, P6, P7,** and **P8** were synthesized as summarized in Schemes 3 and 4; **P10** and **P11** were assembled on a solid support as summarized in Scheme 5.

to form *N*-benzyloxyamides, where powerful acylation methods are necessary. Significant side products due to overreaction or racemization were not observed during purification of the target compounds by HPLC. In addition, two different coupling methods, Fmoc–AA chloride and HATU, were used to synthesize **P9** and both products were identical on HPLC. Nevertheless, further experiments to elucidate possible racemization during synthesis of hydroxamate-containing peptides are required as the proposed mechanism for Fmoc–AA chloride/AgCN involves an oxazolone intermediate[66] usually thought to mediate racemization. Compared with Fmoc–amino acid chlorides, Fmoc–amino acid fluorides possess some advantages due to their stability, their lack of conversion to oxazolones in the presence of tertiary amines, and their ability to affect acylation in the total absence of base.[80] Fmoc–AA fluorides may be an alternative method of choice for both efficient acylation of benzyloxyamino groups on a solid support and minimization of racemization, and should be explored Noteworthy, after deblocking the *O*-benzyl protecting groups, the crude products also contained the species $[M\text{-}16+H]^+$ in their ES-MS spectra, presumably from overreduction of the desired products to their corresponding amide analogs, especially noted in the synthesis of the *N*-benzyloxy-glycine-based **P1** in Table I. This side reaction,[81] which both decreases yields and complicates purification, may be overcome using alternative synthetic strategies with different protection of the *N*-hydroxyl groups.[71,72]

METAL-BINDING PROPERTIES

It is well known that hexadentate trishydroxamate compounds are good ligands for iron coordination based on the discovery and characterization of siderophores, natural products used to facilitate ferric ion uptake by microorganisms, such as DFO. Thus, it was logical to screen the *N,N′*-dihydroxypeptides for their iron-binding properties and metal-binding selectivities. The soft nature of electrospray ionization makes ESI-MS a powerful tool for studying noncovalent interactions[73–75] including ligand–metal coordination. ESI-MS was used as a fast screening method to evaluate metal-binding of *N*-hydroxyamide peptides, while other characterization techniques including HPLC, uv-vis, and NMR were used in addition to gain a more comprehensive knowledge of their properties as metal ligands.

Fe(III) BINDING PROPERTIES

ESI-MS Analysis

Typically, solutions (200 μL) of a peptide ligand (100.0 μM) and different equivalents of $Fe(NO_3)_3$ in methanol were subjected to ESI-MS analysis. All positive-ion ESI-MS were collected under the same conditions (see the experimental section) established to produce singly charged species $[LH]^+$ or $[LNa]^+$ of all free peptide ligands with high abundances. Figure 2 showed the effects of addition of Fe(III) on the ESI-MS of compounds **P7–P9.** No significant abundances of free ligand peaks remained in the spectra upon addition of Fe(III) (1.2 equiv) and the spectra were especially clean. The respective base peaks at ***m/z 644.30, 960.73,*** and ***942.73*** were readily interpreted as the singly charged ions resulting from their coordination with Fe(III), i.e., $[L + Fe\text{-}2]^+$. These results indicated that Fe(III) complexes of **P7–P9** could be readily detected in the gas phase by ESI-MS.

Titration with Fe(III) further revealed the binding stochiometries of compounds **P7–P9.** The ESI-MS obtained usually contained multiple peaks that arose from ionizations of free ligands, metal complexes, and related molecular fragments. It is difficult to calculate the relative concentrations due to possible differences in ionization, and thus the binding constants K_c were only estimated. As shown in Figure 3, the relative abundance in each ESI-MS as a factor instead of K_c served to evaluate the relative metal-binding affinity of each compound. Relative abundance was calculated based on the percentage of the resulting singly charged species $[LM]^+$ to the total observed free ligand-related peaks including $[LH]^+$, $[LNa]^+$, and $[LH_2]^{2+}$ by the following equation:

$$L + M^{n+} \rightleftharpoons LM^{n+}$$

$$K_c = [LM^{n+}] / [L][M^{n+}]$$

$$\text{Relative abundance} = [LM^{n+}] / \{[LM^{n+}] + [LH]^+ + [LNa]^+ + [LH_2]^{2+}\} (\%)$$

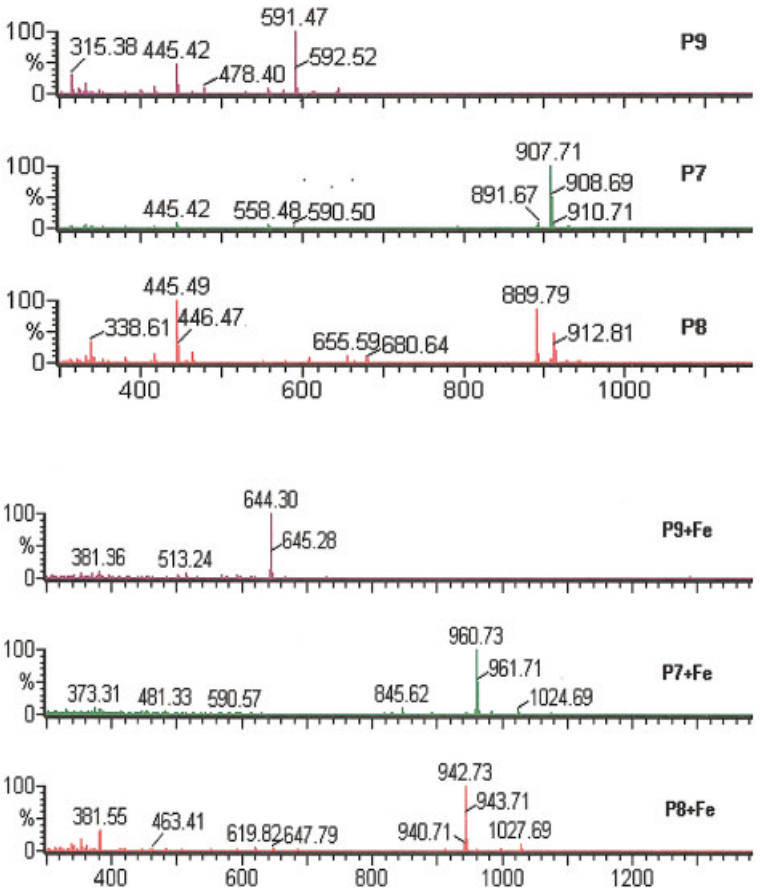

FIGURE 2 Positive-ion ESI-MS for the dihydroxypetide ligands **P7–P9** (100 μM) with 1:0 and 1:1.2 mole ratios of $Fe(NO_3)_3$ in CH_3OH. The singly charged peak **[L + Fe-2]**$^+$ indicated the formation of their Fe(III) complexes in the gas phase.

Figure 3 clearly showed the dependence of the relative abundances of complex upon added Fe(III) concentration. As the concentration of Fe(III) increased, the relative abundances of the singly charged species $[L@Fe]^+$ increased, and the relative abundances of the singly charged species $[LH]^+$ of the three compounds decreased correspondingly. As for both **P7** and **P8,** complexation with Fe(III) was nearly complete upon addition of 1.2 equiv Fe(III).

In contrast, compounds **P3, P5,** and **P6** generated complicated spectra upon the addition of Fe(III). Figure 4 shows the spectra of **P3, P5, P6,** and their coordination with 1.2 equiv of Fe(III). The lowered abundances of species $[LH]^+$ clearly indicated that these compounds participated in coordination with Fe(III). As for **P3 and P5,** species from intramolecular coordination and intermolecular coordination showed similarly significant abundances. As for **P6,** a species of bimolecular coordination was observed, but no significant species of intramolecular coordination was apparent. The type of coordination correlated with Fe(III) concentration. Compared to the desired intramolecular coordination, bimolecular coordination prevailed at 0.4 equiv of Fe(III). As the Fe(III) concentration was further increased, the spectra became more complicated, and both intramolecular and bimolecular coordination were apparent. Compared to Fe(III) coordination of **P7–P9,** results with **P3, P5,** and **P6** clearly showed the impact of ligand structure on the metal-binding property as revealed by ESI-MS.

To further compare the relative Fe(III) binding affinity of ligands, competition experiments were performed. All ESI-MS were recorded for solutions of two different peptide ligands (100 μM of each ligand) in CH_3OH pretreated with 1 equiv $Fe(NO_3)_3$. By comparing the relative abundances of the resulting intramolecular Fe(III) complex species to their corresponding free ligand in their ESI-MS (Figure 5), the relative binding affinities of compounds in the following order—**P7** > **P9, P5** > **P6, P4** > **P3, P8** > **P7, P8** > **P9, P8** > **P6,** and **P7** > **P5**—were estimated.

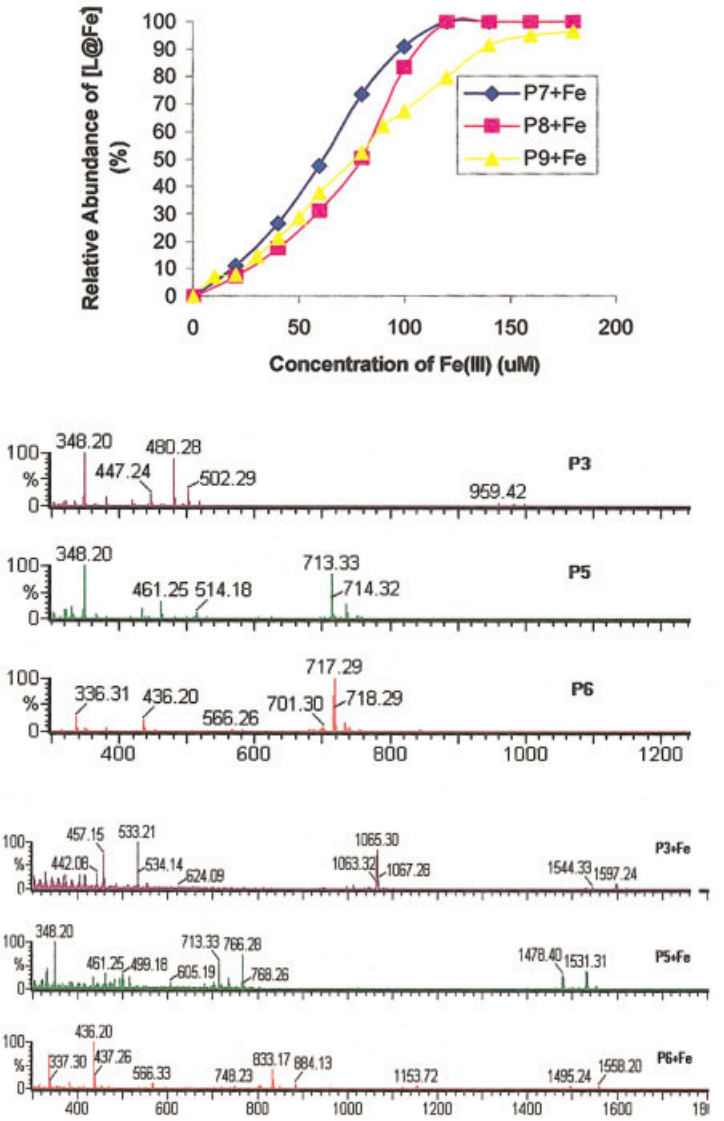

FIGURE 3 The titrations of compounds **P7–P9** (100 μM) with $Fe(NO_3)_3$ in CH_3OH, showing the dependence of the relative abundances of the singly charged species $[L+Fe\text{-}2]^+$ in their ESI-MS on the added Fe(III) concentration.

HPLC Analysis

ESI-MS only reflects the relative compositions of the ion species for ligand–metal coordination in the gas phase. To ascertain coordination of *N,N′*-dihydroxypeptides with Fe(III) in solution, all solutions prepared for ESI-MS were also subjected to HPLC analysis. Figure 6 shows HPLC profiles of three representative compounds **P7–P9.** The addition of Fe(III) to compound **P9** only produced a minor new peak at 13.2 min. Compared to **P9,** the addition of Fe(III) to compound **P7** (peak at 14.4 min) produced a new peak of higher abundance at 16.4 min. Nevertheless, instead of the free-ligand peak of **P8** at 18.1 min, a new broad peak was eluted at 23.2 min upon addition of Fe(III). After isolation by semipreparative HPLC and analysis by ESI-MS these new peaks were related with the desired Fe(III) complexes as showed in Figure 2. The high Fe(III)-binding affinity of **P7–P9** allowed the resulting complexes to be separated from free ligands by HPLC. The relative area of new peaks to free ligand peaks clearly reflected the relative stabilities of the resulting Fe(III) complexes in solution phase in the following order—**P8** > **P7** > **P9**—consistent with the observation from ESI-MS. Obviously, HPLC is a convenient method to evaluate the relative ligand properties of *N,N′*-dihydroxypeptides in solution.

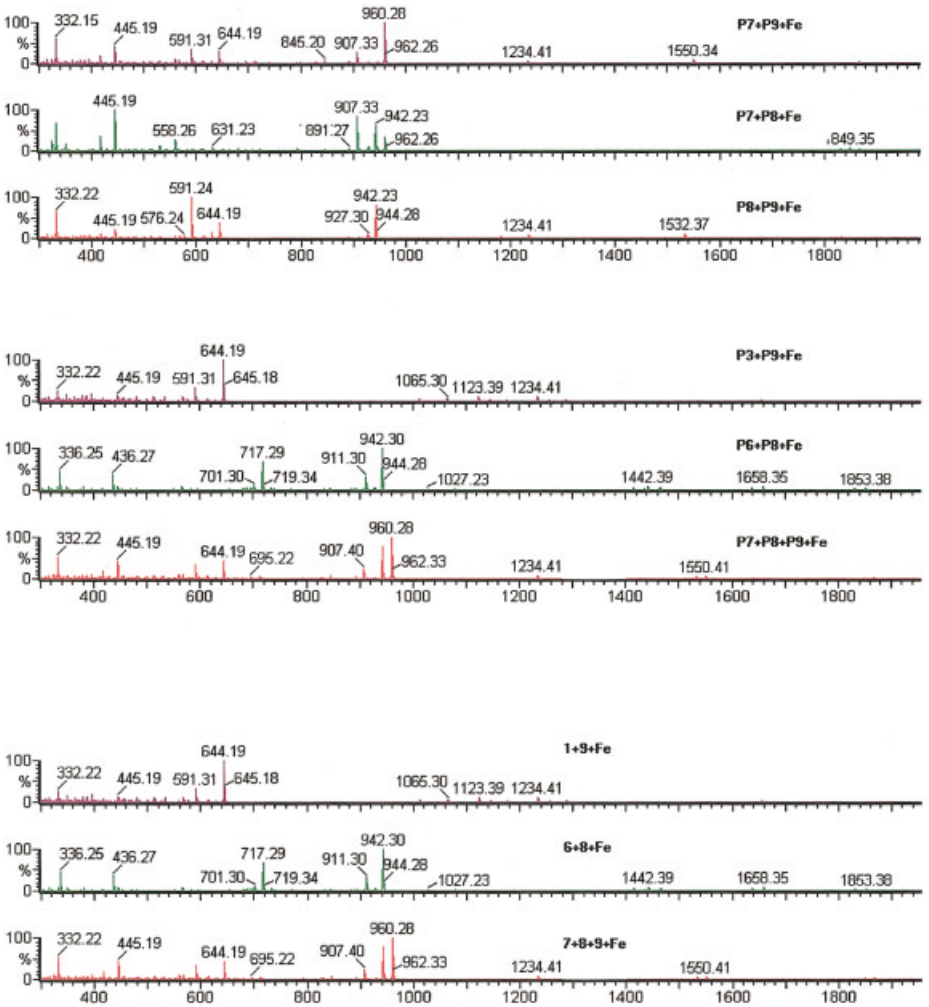

FIGURE 4 Positive-ion ESI-MS for the solutions of *N,N′*-dihydroxypeptide ligands **P3, P5,** and **P6** (100 μM) with different mole ratios of $Fe(NO_3)_3$ in CH_3OH, showing the spectral complexity upon the addition of Fe(III).

UV-Vis Spectroscopy

UV-vis spectroscopy has been widely used to study complexation of hydroxamates with Fe(III). A typical 1:3 complex such as ferrioxamine B shows maximum absorption (λ_{max}) at 420 nm while a 1:1 complex of a monohydroxamic acid with iron (III) at low pH has a λ_{max} at 520 nm. A 1:2 complex formation was identified with λ_{max} at 466 nm observed during transformation of a 1:3 complex to a 1:1 complex.[7,13,26] Similarly, coordination of *N,N′*-dihydroxyamide pep-

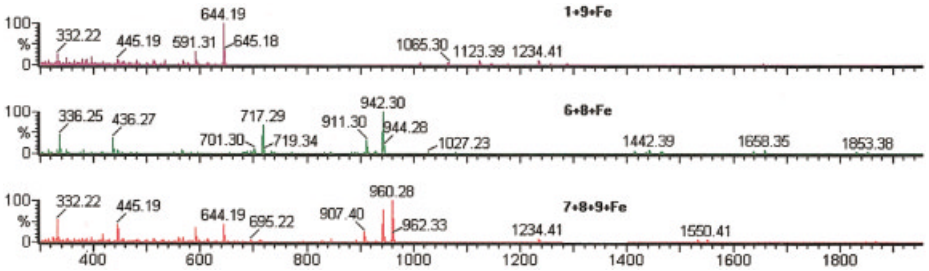

FIGURE 5 Positive-ion ESI-MS for the competition solutions of different dihydroxypeptide ligands **P3** and **P6–P9** (100 μM) with 1 equiv of $Fe(NO_3)_3$ in CH_3OH.

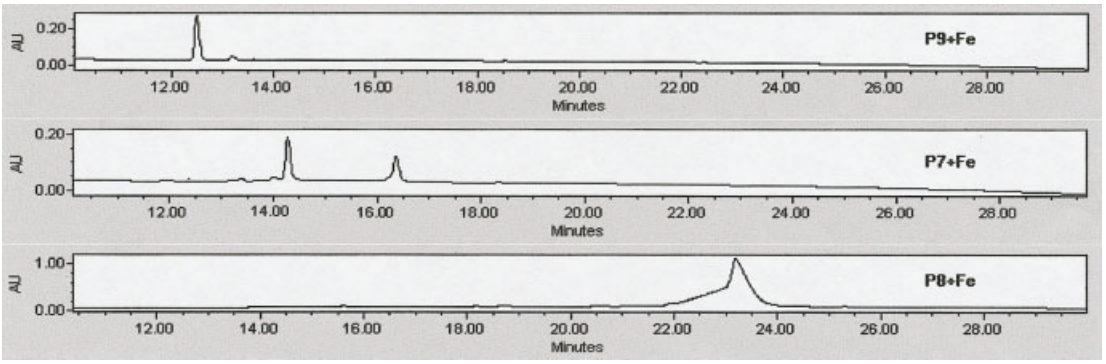

FIGURE 6 The HPLC profiles for solutions of **P7–P9** containing 3 equiv Fe(III), showing the existences and relative stabilities of their Fe(III) complexes in HPLC mobile phase. The HPLC analysis is performed on a Vydac C-18 column using a linear gradient of 0.1% TFA in H_2O and 0.1% TFA in CH_3CN and from 90:10 to 10:90 over a period of 30 min, flow rate 1.0 mL/min, detection at 220 nm. Complexes were confirmed by ESI-MS of HPLC peaks.

tides with Fe(III) increased absorption at wavelengths ranging from 420–520 nm. For peptides **P7–P9,** the λ_{max} were 474, 446, and 458 nm, respectively (Figure 7) within the reported range for 1:2 complexes.

Titration with Fe(III) showed that the absorption intensities were dependent upon the Fe(III) concentration, and reached equilibrium near 1 equiv for **P7** and **P8,** but requiring approximately 3 equiv for **P9.** These characteristic peaks could be applied to both qualitative and quantitative identification of complex formation. It is noteworthy that the addition of Fe(III) also significantly enhanced the absorption in the uv region significantly and was accompanied by a shift of λ_{max} to longer wavelength (226 nm).

^{1}H-NMR Spectroscopy

^{1}H-NMR experiments were undertaken to further characterize the metal-binding properties of representative compound **P8** with higher affinity to reduce presence of free ligand, especially the effect of metal coordination on the structure (conformation) of **P8.** Ga(III) possesses similar coordination properties as Fe(III), and has been used as a surrogate of Fe(III) in ^{1}H-NMR experiments. Studies via ESI-MS analysis confirmed that coordination of 8 with Ga(III) was very similar to Fe(III). Therefore, the Ga(III) complex of **P8** was prepared by mixing 2.0 equiv of $Ga_2(SO_4)_3$ with compound **P8** in CH_3CN/H_2O(3:2) and stirring overnight. The resulting complex was lyophilized, confirmed by HPLC and ESI-MS (*m/z* 955.47), and dissolved in DMSO-d_6 for ^{1}H-NMR experiments. Proton chemical shifts of **P8** were assigned by analysis of correlated spectroscopy (COSY), total COSY (TOCSY), and nuclear Overhauser effect spectroscopy (NOESY) spectra. Only Ala and Leu have spin propagation from the amide NH through the α, β, γ, and δ protons [Figure 8(b)]. Correlated proton resonances from 1.3 to 5.2 ppm in Figure 8(a) were unambiguously assigned to β, γ, and δ resonances of (NOH)Phe and Pro residues. Observed sequential $\alpha(i)$–NH(i + 1) NOE, such as Phe$^{(NOH)}$–Ala and

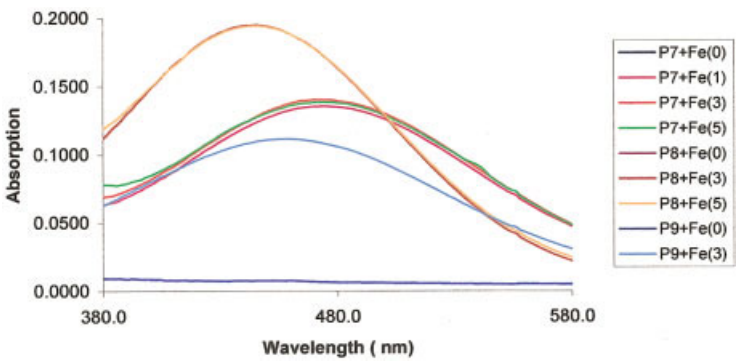

FIGURE 7 UV-visible spectra for coordination of **P7–P9** with 1, 3, and 5 equiv of Fe(III) in CH_3CN/H_2O (7:3).

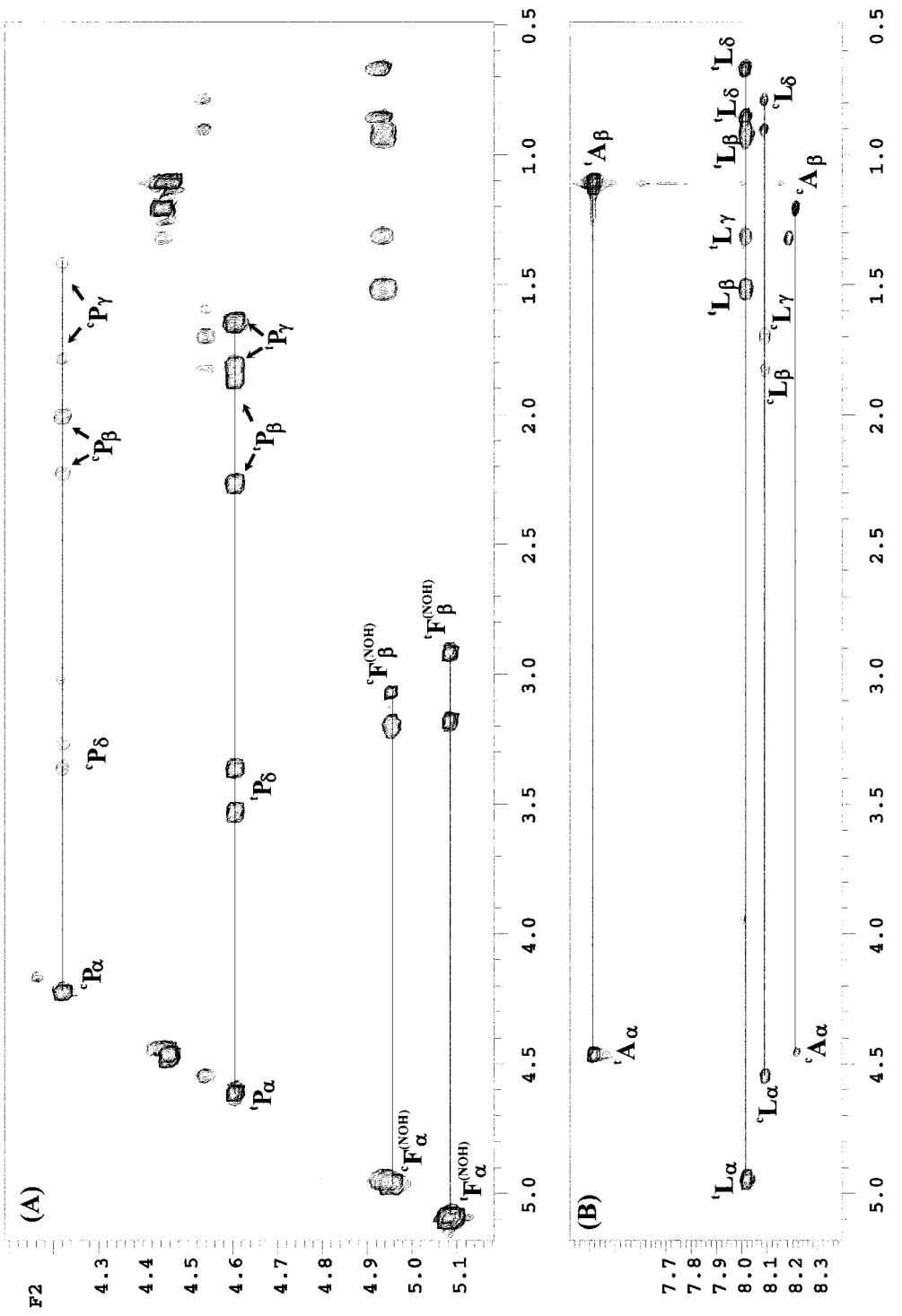

FIGURE 8 Expansion of (a) Hα-aliphatic and (b) NH-aliphatic region of 600 MHz TOCSY spectra of **P8** cyclo(Leu–Ψ[CON(OH)]Phe–Ala–Pro)$_2$ in DMSO-d$_6$.

Pro–Leu cross peaks in Figure 9(b), further confirmed the (NOH)Phe–Ala and Pro–Leu connectivities, respectively. The presence of proline in **P8** resulted in *cis/trans*-isomerization of the Ala–Pro amide linkage. This was reflected by two observed sets of chemical shifts for each individual proton resonance in one-dimensional (ID) (Figure 10) and two-dimensional (2D)-TOCSY spectra (Figure 8). Correlated Pro(α–β–γ–δ) spin propagation was used to further differentiate the *cis/tran*-isomers, thus two groups of the correlated-cross peaks, from 4.61 to 1.65 ppm and from 4.22 to 1.43 ppm, shown in Figure 8(a) were related to different isomers. Furthermore, a strong NOE cross peak between Ala-α (4.47 ppm) and Pro-δ (3.36 and 3.54 ppm) [$^{t}A\alpha$–$^{t}P\delta$ in Figure 9(a)] indicated a *trans*-Ala–Pro amide linkage while an observed Ala-α (4.46ppm)–Pro-α (4.22ppm) cross peak [$^{c}A\alpha$–$^{c}P\alpha$ in Figure 9(a)] suggested a *cis*-amide conformation. **P8** revealed a symmetrical spectra pattern and the observed Phe$^{(NOH)}$-Leu α NOE cross peak [Figure 9(c)] confirmed the presence of the hydroxamate group in **P8.** All sequential connections between adjacent residues were observed and the continuous path shown in Figure 9 indicated a cyclic [Leu–Phe$^{(NOH)}$–Ala–Pro] segment in **P8.** Complete assignments of proton resonance for each residue are available in Table II. The population of *cis/tran*-conformers estimated from 1D spectrum was approximately 20/80%.

The coordination geometry of **P8** was investigated by TOCSY and NOESY spectra of the Ga(III)–**P8** complex. The disappearance of the N–OH resonance (such as peaks at 9.08 and 10.24 ppm in Figure 10) indicated complex formation between Ga(III) and the Leu(CO)–(NOH)Phe hydroxamate group. Of particular interest are the observed upfield shifts of Leu-α,β and (NOH)Phe-α resonances [Figure 11(a)]. The Ga(III)–**P8** complex induces a *cis*-amide linkage between Leu and (NOH)–Phe to position the hydroxamate oxygens in a bidentate orientation, as evidenced by the observed strong Leu-α-(NOH)Phe-α NOE cross peak [Phe$^{(NOH)}$-α–Leu-α in Figure 11(b)]. The resulting *cis*-conformation brings the (NOH)Phe aromatic ring in close proximity to the Leu residue leading to the upfield Leu-α [at 4.09 ppm in Figure 11(a)] and Leu-β [at -0.59 ppm in Figure 11(a)] shifts due to the shielding from the aromatic ring. As previously reported,[46,53,76] a Ga(III)–peptide complex may adopt stable C-*cis* or N-*cis* series of isomers of the Ga–hydroxamate Δ configuration, depending on whether the C atom of the hydroxamate group is above the N atom, and on whether the five-membered Ga(III)–hydroxamate rings has the same (*cis*) or opposite (*trans*) orientation. In case of Ga(III)–**P8** complex, the number of isomers may increase due to *cis/trans*-conformers of the Ala–Pro amide linkage. The complicated NOE spectra precluded detailed conformational analyses for each isomer. However, the richness of NOE cross peaks in Figure 11(b) and 11(c) indicated the Ga(III)–**P8** complex probably has several well-defined conformations due to different interactions of Ga(III) and the ligand in different complexes.

Metal-Binding Selectivities

As identified by ESI-MS, compounds **P7–P9** exhibited high affinity for intramolecular coordination with Fe(III). These compounds were further screened for their binding properties towards other metals of medical interest. Initially, solutions of **P3** and **P7–P9** (100 μM) in methanol were pretreated with 1.2 equiv amount of different metals including Fe(III), Ga(III), Fe(II), Cu(II), Co(II), Mn(II), Ni(II), and Zn(H). The relative abundances vs different metals plots were showed in Figure 12.

Based on the relative abundance, it was found that compounds **P7–P9** exhibited high preference for intramolecular coordination with Fe(III) and Fe(II). Compared to Fe(II) and Fe(III), **P7** and **P9** showed medium affinities for Ga(III) and Cu(II), and weaker affinities for Mn(II), Ni(II), and Zn(II). Interestingly, compound **P8** showed higher affinities for all metal ions than **P7** and **P9.** The relative binding affinities of **P3** towards all the tested metals for 1:1 complexation were remarkably low. Competition experiments by ESI-MS analysis were performed to further confirm metal-binding selectivity. Therefore, solutions of compound **P8** (100 μM) in methanol were similarly pretreated with equimolar amounts of two different metals. By comparing the relative abundances of the resulting two complex species in the ESI-MS, the relative metal binding affinities of **P8** were displayed in the following order—Ga(III) > Fe(III) > Fe(II) > Cu(II) > Co(II) > Mn(II) > Ni(II) > Zn(II)—similar to the observation above (Figure 12). Finally, solutions of compounds **P7–P9** (100 μM) in CH_3CN/H_2O (7:3) were pretreated with a mixture of different metals (100 μM of each metal ion) including Fe(III), Cu(II), Ni(II), Co(II), Mn(II), and Zn(II). Just like the spectra in Figure 2, the only observed singly charged species of high abundance were $[Fe + L\text{-}2]^+$ (Figure 13). It is likely that differences observed between different experiments reflect differences in ionization and possible presence of additional complexes.

Thus, *N,N′*-dihydroxypeptides such as compounds **P7–P9** can be categorized highly selective for Fe(III) over Cu(II), Co(II), Mn(II), Ni(II), and Zn(II).

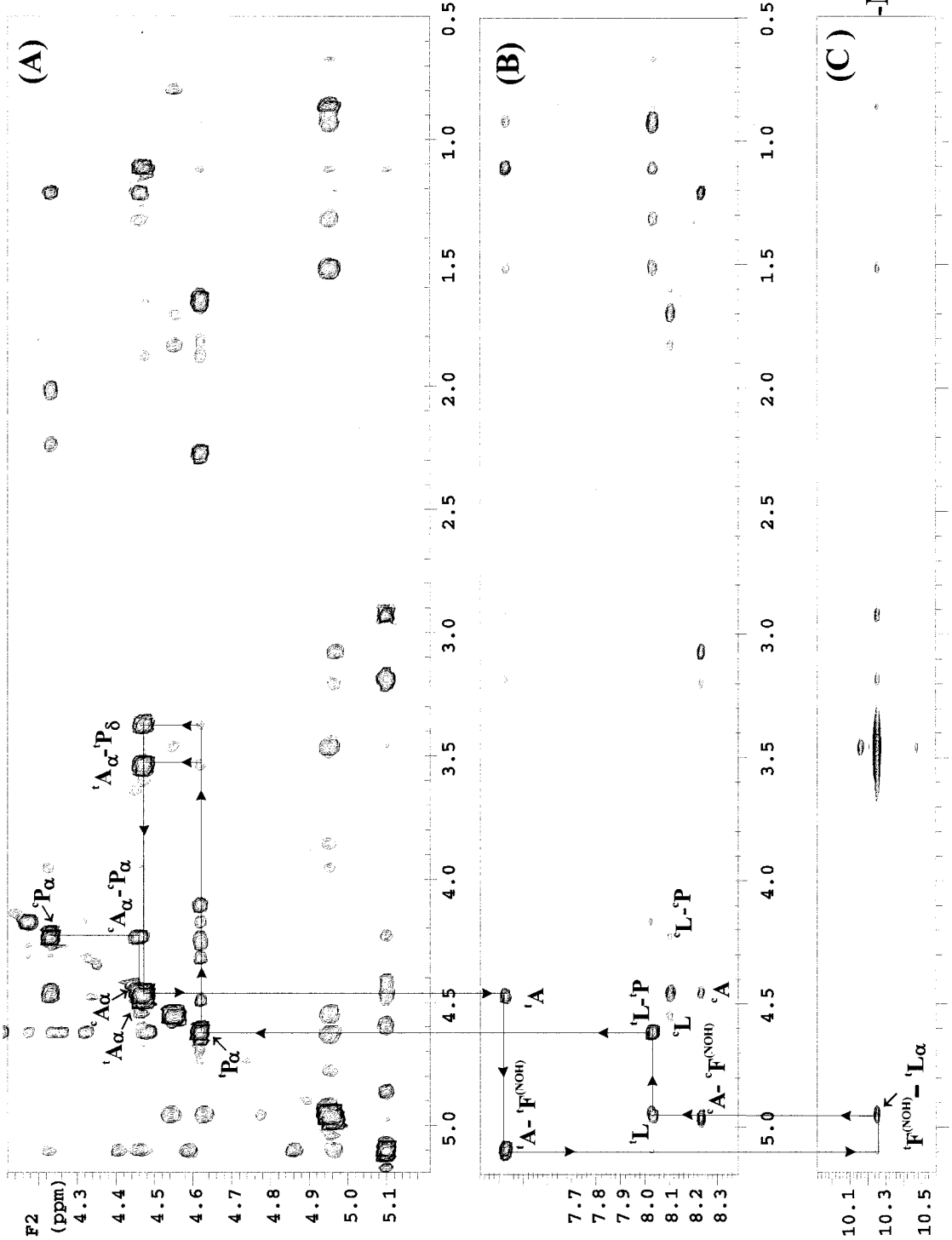

FIGURE 9 Expansion of (a) Hα-aliphatic, (b) NH-aliphatic, and (c) NOH-aliphatic region of 600 MHz NOESY spectra of **P8** cyclo(Leu–Ψ[CON(OH)]Phe–Ala–Pro)$_2$ in DMSO-d_6. Cross peaks of the continuous sequential path for residues between Leu and Pro are indicated.

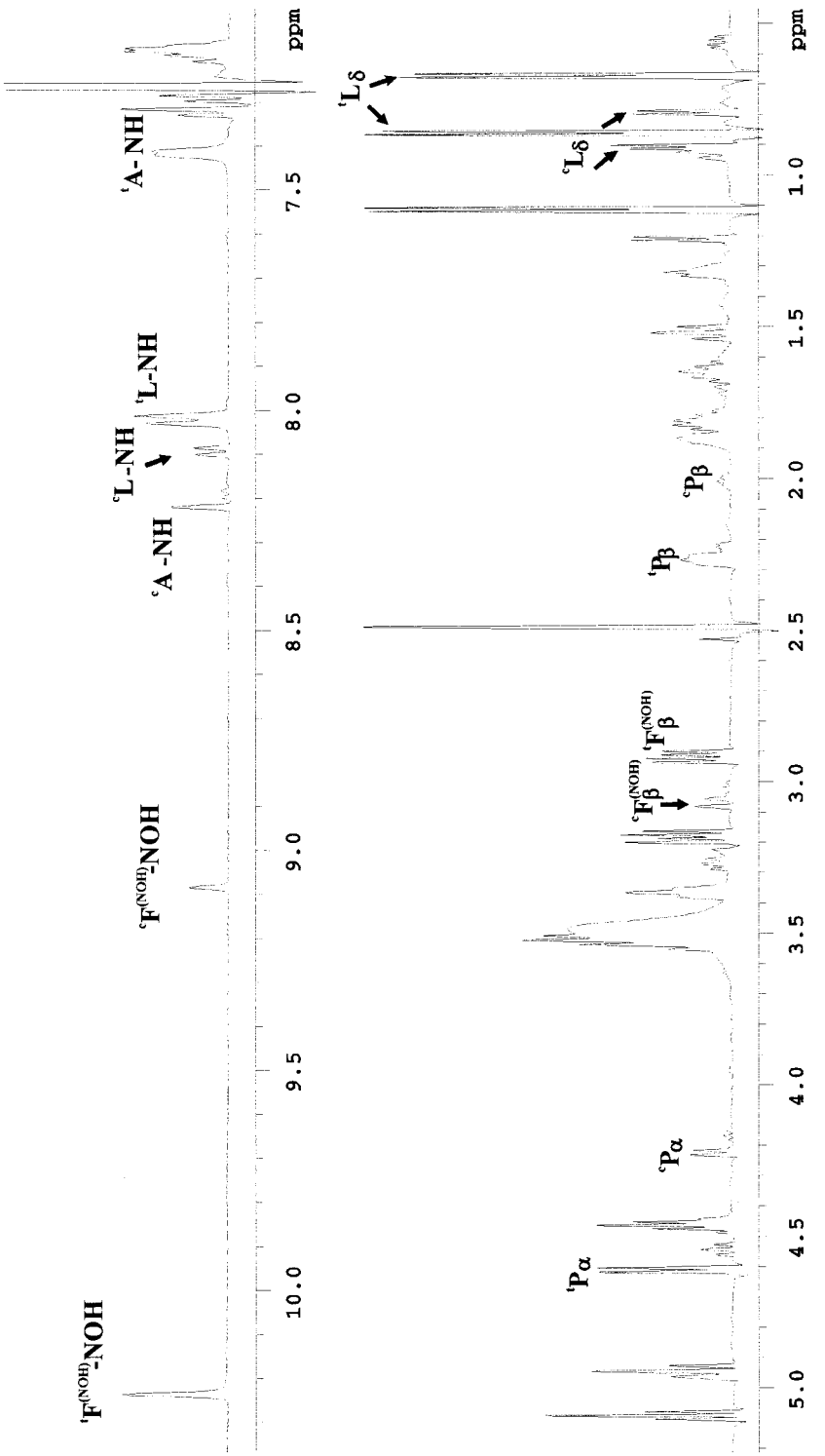

FIGURE 10 The 600 MHz proton spectrum of **P8** cyclo(Leu–Ψ[CON(OH)]Phe–Ala–Pro)$_2$ in DMSO-d$_6$.

Table II Proton Chemical Shifts (ppm) of P8 ***trans*-cyclo(Leu–Ψ[CON(OH)]Phe–Ala–Pro)$_2$ in DMSO**[a]

	NH	αH	βH	Others
Leu	8.02	4.95	1.52, 0.92	γ 1.32; δ 0.87, 0.67
	(8.09)	(4.55)	(1.83, 1.70)	(γ 1.60; δ 0.90, 0.79)
(NOH)Phe		5.09	3.18, 2.93	NOH 10.24
		(4.96)	(3.20, 3.07)	(NOH 9.08)
Ala	7.42	4.47	1.11	
	(8.21)	(4.46)	(1.22)	
Pro		4.61	2.27, 1.87	γ 1.82, 1.65; δ 3.54, 3.36
		(4.22)	(2.23, 2.01)	(γ 1.79, 1.43; δ 3.36, 3.27)

[a] Numbers in parentheses are the chemical shifts of the *cis*-isomer.

RELATION BETWEEN STRUCTURE AND METAL BINDING

As described above, the metal-binding properties of *N,N′*-dihydroxypeptides have been evaluated by ESI-MS, HPLC, uv-vis, and ^{1}H-NMR. Even though the results are qualitative, they can assist in understanding the relationship between structure and metal binding.

The Metal-Binding Selectivity of *N,N′*-Dihydroxypeptides

As exemplified by **P8,** *N,N′*-dihydroxypeptides showed high binding selectivities for Fe(III) over Cu(II), Mn(II), Zn(II), Ni(II), and Cd(II). The high selectivities can be ascribed to the two hydroxamate groups that provide hard donors of negatively charged oxygen for the hard acidic Fe(III). The affinity of *N,N′*-dihydroxypeptides for Fe(III) complex formation is in accordance with the Hard and Soft Acid and Base (HSAB) principles of Pearson.[77,78]

The Effects of Linker Length on Fe(III) Coordination Mode

ES-MS analysis indicated clearly that compounds **P7–P9,** had higher tendencies for forming 1:1 intramolecular complexes with Fe(III) in the gas phase than compounds **P3, P5, P6,** and **P12.** These tendencies reflected the importance of linker length in determining Fe(III) coordination mode and binding affinity. As we have seen with compounds **P7–P9,** a two α-amino acid spacer between the amino acids bearing the *N*-hydroxyl groups, i.e., a spacer of 10 α-amino acid atoms between the two hydroxamates, or even longer linker, provides enough conformational flexibility and suitable orientations for both hydroxamate groups to match both geometrical and electronic requirements of Fe(III) coordination. Adversely, a shorter linker such single amino acid spacer as seen in compounds **P3, P5, P6,** and **P12** led to unfavorable intramolecular coordination with Fe(III) and intermolecular coordination became competitive (Figure 14). There were a variety of other peaks present in the spectra of compounds **P3, P5, P6,** and **P12** that could not be assigned completely, suggesting that iron coordination may generate additional higher coordination species, or may promote fragmentation of ligands during the process of mass spectrometry.

It is significant to identify suitable linkers connecting the two hydroxamates that may be the structural determinants for forming thermodynamically stable Fe(III) complexes. Caudle et al.[45] used ES-MS to show conclusively that for dihydroxmate ligands with a methylene-bridge linker; the $n = 8$ species forms monomer whereas the $n = 2$ species forms a dimer. The naturally occurring nonpeptidic Tris-hydroxamate siderophore, desferrioxamine, possesses a high Fe(III) binding constant and the linker between the two hydroxamates is 9 atoms. The Akiyama group reported the design and synthesis of DFO-mimicking trihydroxamate-containing peptides with a ten-atom[41] spacing between two hydroxamates consistent with our observation on dihydroxamate-containing peptides. We have constructed Fe(III)-binding trihydroxypeptides with high affinity based on the above results.[4]

The Effects of Backbone Cyclization on Metal-Binding Properties

ESI-MS-based competition experiment and HPLC analysis confirmed that the relative Fe(III) binding affinities of **P8** is higher than **P7.** As shown in Figure 12, compound **P8** actually exhibited higher binding affinities than **P7** to all metals tested. These results suggest that the advantages of a macrocyclic effect including preorganization and favorable enthropic contributions[79] may prevail against possible cyclization-induced disadvantages including losses of poten-

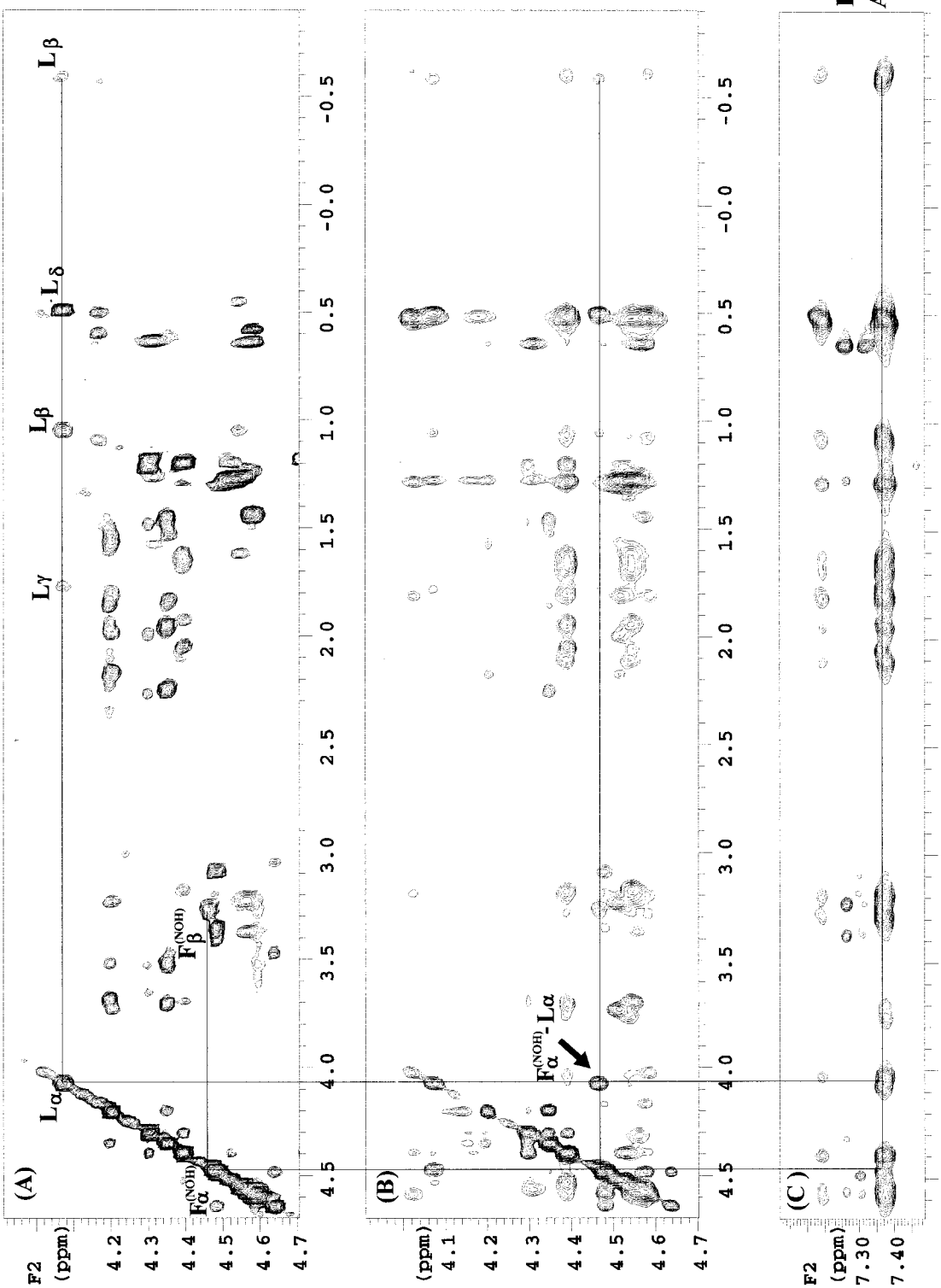

FIGURE 11 Expansion of (a) Hα-aliphatic region of 600 MHz TOCSY, (b) Hα-aliphatic, and (c) N(OH)Phe, aromatic–aliphatic region of 600 MHz NOESY spectrum of Ga(III)–P8 Ga(III)–cyclo(Leu–Ψ[CON(OH)]Phe–Ala–Pro)$_2$ complex in DMSO-d_6.

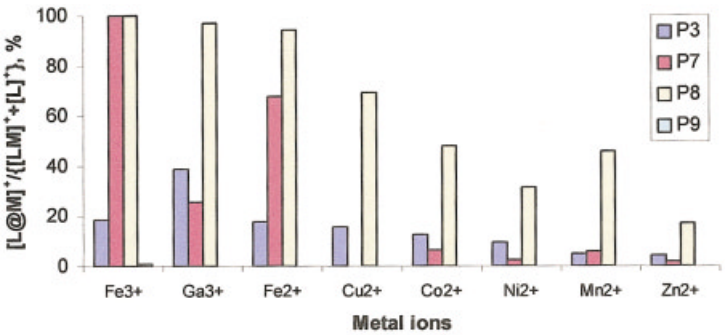

FIGURE 12 The relative ion abundances {$[L + M]^+/ ([L + M]^+ + [L]^+)$, %} obtained from positive-ion ESI-MS for 1:1 metal complexes of compounds **P3,** and **P7–P9** (100 μM) at a metal-to-ligand ratio of 1.2:1 in methanol, showing the high selectivity of *N,N′*-dihydroxypeptides of this type for coordination with Fe(III) among the 9 different metals tested.

tial metal-binding sites (N-terminal amino group and C-terminal carboxylic acid), decreased conformational flexibility, and increased steric strain.

Cyclization has widely been used as a strategy for studying the bioactive conformation and in the discovery of peptidomimetics. Improvements in biological potency, receptor selectivity, metabolic stability, and bioavailability have also been reported. As exemplified by **P8,** cyclization can be used as a strategy for preorganizing linear *N,N′*-dihydroxypeptides for improving binding affinity in metal coordination. In contrast, cyclization of **P5** led to the decreased relative binding affinity as seen in **P6,** indicating that cyclization of two hydroxamates connecting with unsuitable length may enhance the unfavorable enthalpic contributions to intramolecular complex formation.

The Cooperation of Two Hydroxamates with Other Metal-Binding Groups

Typically, a Fe(III) complex features an octahedral geometry with 6 ligand atoms. Siderophores of high Fe(III) binding affinities such as DFO contain three bidentate hydroxamate groups. It is suggested that two hydroxamate groups in *N,N′*-dihydroxypeptides cooperate with other groups in complexation such as peptide amide bonds, N- and C-terminal groups, and/or side chains for forming stable Fe(III) complex. This is evidenced by peptide **P7** and **P9. P7** contains a C-terminal carboxylate that is also good ligand for Fe(III) coordination due to its negatively charged oxygen donors, and shows higher Fe(III) binding affinity than peptide **P9.**

The Effects of Neighboring Groups on Fe(III) Binding Affinity

The effects of neighboring groups of hydroxamates on the Fe(III) binding affinity was explored by comparing peptides **P1–P3, P9,** and **P11.** Competition experiments showed the following order: **P1** > **P2,** suggesting that neighboring groups play a significant role in affinity.

The Effects of Metal Coordination on the Structure

NMR spectroscopy showed that coordination of peptide **P8** with Ga(III) caused disappearance of the protons in the *N*-hydroxamate groups, clearly indi-

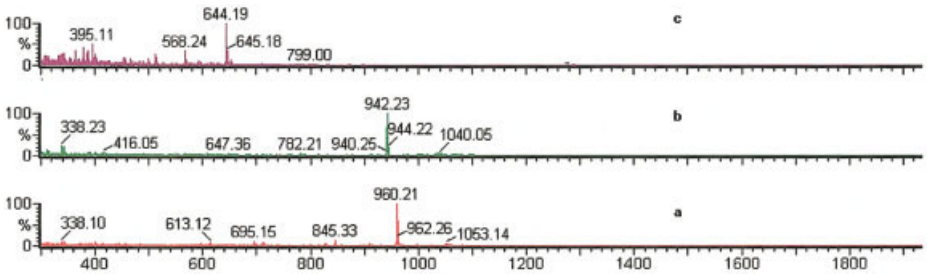

FIGURE 13 ESI-MS: (a) compound **P7** + $Fe(NO3)_3$ + $ZnSO_4$ + $NiCl_2$ + $CuSO_4$ + $Co(NO_3)_2$ + $MnCl_2$; (b) compound **P8** + $Fe(NO3)_3$ + $ZnSO_4$ + $NiCl_2$ + $CuSO_4$ + $Co(NO_3)_2$ + $MnCl_2$; (c) compound **P9** + $Fe(NO3)_3$ + $ZnSO_4$ + $NiCl_2$ + $CuSO_4$ + $Co(NO_3)_2$ + $MnCl_2$ (100 μM of each).

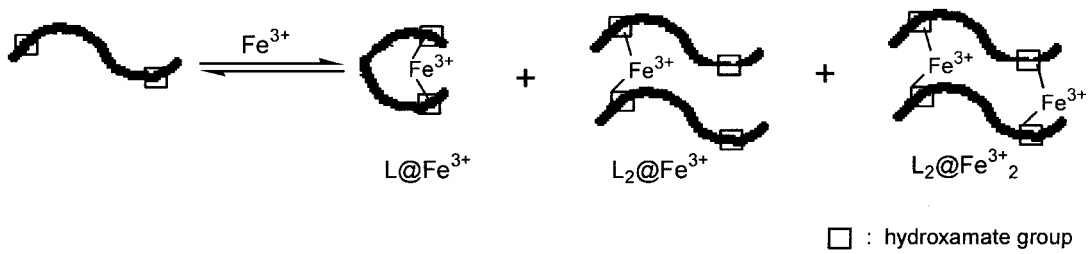

FIGURE 14 Schematic representation of three possible complexes of *N,N′*-dihydroxypeptide ligands with Fe(III). As detected by ESI-MS, the size of the linker between the two hydroxamate groups dominates the coordination mode and a two amino acid linker favors intramolecular coordination.

cating that metal-binding sites are located at the two *N*-hydroxyamides. It also revealed that Ga(III) coordination further defined the structure of the cyclic compound, but that several isomers existed. Leong and Raymond[76] reported that at least **P7** isomers existed in Fe(III) trihydroxamate complexes due to different wrapping of the linear chain that positions the hydroxymate group as well as alternative orientations of the hydroxamates as bidentate ligands. As pointed out early,[3] multiple isomers of metal–ligand complexes may lead to ambiguous interpretations regarding the conformation of the complex responsible for observed activity. Nevertheless, multiple conformers from metal coordination also generate molecular diversity with enhanced potential for sampling biologically relevant conformations in the context of a combinatorial library.

Comparing the different methods of analysis used, ESI-MS showed advantages in characterizing a series of ligands for metal coordination. Among them, direct observation of complex speciation and ready comparison of relative ligand affinity by ESI-MS were significant, supporting the use of ESI-MS for screening metal-binding libraries. It is widely recognized that gas-phase information obtained from ESI-MS accurately reflects noncovalent reactions in solution, but it is noteworthy that different analytical methods may lead to different observations due to different conditions for analysis. For example, compared to high concentrations used in NMR studies, the low concentration of ligands in the gas phase for ESI-MS might minimize intermolecular reactions. Moreover, solubility is an important factor in ESI-MS analysis that may preclude identification of some metal complexes insoluble in aqueous methanol or acetonitrile solutions. For a comprehensive understanding of ligand behavior in metal coordination, a combination of different analytic approaches remains essential.

CONCLUSIONS

Peptide amide bonds were successfully modified to bear *N*-hydroxyl groups for metal coordination. An array of model *N,N′*-dihydroxypeptides were designed and synthesized for probing the relation between structure and metal binding. The strategies for synthesis both in solution and solid support presented here are amenable to the construction of metal-binding peptides libraries. As demonstrated by ESI-MS, high iron-binding affinity and selectivities were attainable with *N,N′*-dihydroxypeptides. Compounds **P8** and **P9** are two representatives of *N,N′*-dihydroxypeptides capable of forming complexes with Fe(III) with high affinity and selectivity due to coordination of the bidentate hydroxamate groups with Fe(III) consistent with ligand architecture. Cyclic compound **P8** is especially attractive as a robust and compact metal-binding scaffold for combinatorial chemistry. By variation of the amino acid residues, a metal-binding library could be constructed utilizing this scaffold. Moreover, the structure-metal binding relationship revealed here should facilitate further molecular design and fine-tuning of novel metal-binding ligands with altered or enhanced function.

EXPERIMENTAL

General

^{1}H-NMR spectra were recorded on Varian HG-300 (300 MHz) or Varian Inova-600 (Varian Inc., Palo Alto, CA) spectrometer (Table III). Routine positive ESI-MS experiments were performed on a Waters ZQ mass spectrometer at cone voltage 60 kV. For all measurements, the test solutions were injected at a flow rate of 10 μL/min for 2 min. UV/vis measurements utilized a Cary model 3E spectrophotometer. Chromatographic purifications were performed by

Table III Some ^{1}H-NMR Data for the Key Intermediates and Final Products

	P3: H–Val–Ψ[CON(OH)]–Phe–Ala–Leu–NHOH				
	NH	Hα	Hβ	Hγ	Hδ
Val		4.1	2.4	0.98, 0.82	
Phe		5.09	3.18, 3.09		
Ala	8	4.31	1.18		
Leu	7.99	4.19	1.51	1.4	0.87, 0.83
	P1: H–Val–Ψ[CON(OH)]–Gly–Ala–Leu–NHOH				
	NH	Hα	Hβ	Hγ	Hδ
Val	8.06	4.14	2.33	1.00, 0.90	
Gly		4.36, 4.11			
Ala	8.14	4.34	1.16		
Leu	8	4.18	1.51	1.4	0.85
	P2: H–Val–Ψ[CON(OH)]–Ala–Leu–NHOH				
	NH	Hα	Hβ	Hγ	Hδ
Val1		4.14	2.34	1.01, 0.88	
Ala2		4.85	1.33		
Ala3	7.73	4.28	1.16		
Leu4	7.96	4.17	1.5	1.4	0.84
	P4: H–Val–Ψ[CON(OH)]–Phe–Ala–Pro–Leu–NHOH				
	NH	Hα	Hβ	Hγ	Hδ
Val1		4.09	2.34	0.97, 0.82	
Phe2		5.12	3.18, 3.07		
Ala3	8.26	4.53	1.2		
Pro4		4.29	1.96, 1.86	1.78	3.47
Leu5	7.83	4.14	1.55	1.42	0.85
	P5: H–Leu–Ψ[CON(OH)]–Phe–Ala–Leu–Ψ[CON(OH)]–Phe–Ala–OH				
	NH	Hα	Hβ	Hγ	Hδ
Leu1		4.12	1.72	1.44	0.87
Phe2		5.08	3.15, 3.09		
Ala3	8.01	4.33	1.15		
Leu4	7.77	4.94	1.57	1.29	0.86
Phe5		5	3.10, 3.07		
Ala6	8.02	4.22	1.27		
	P6: cyclo[Leu–Ψ[CON(OH)]–Phe–Ala–]$_2$				
	NH	Hα	Hβ	Hγ	Hδ
Leu	7.72	4.71	1.47, 1.42	1.11	0.82
Phe		4.81	3.11, 3.01		
Ala	7.51	4.17	1.21		

Table III (*Continued*)

	P7: H–Leu–Ψ[CON(OH)]–Phe–Ala–Pro–Leu–Ψ[CON(OH)]–Phe–Ala–Pro–OH				
	NH	Hα	Hβ	Hγ	Hδ
Leu1	8.04	4.14	1.72, 1.45	1.45	0.87
Phe2		5.09	3.16, 3.08		
Ala3	8.22	4.52	1.19		
Pro4		4.21	2.11, 1.88	1.88, 1.84	3.56, 3.48
Leu5	7.68	4.89	1.59, 1.49	1.27	0.83
Phe6		4.99	3.11, 3.03		
Ala7	7.81	4.52	1.18		
Pro8		4.36	1.93	1.84, 1.75	3.51
	P9: H–Leu–Ψ[CON(OH)]–Phe–Ala–Pro–Leu–OH				
	NH	Hα	Hβ	Hγ	Hδ
Leu1	8.03	4.14	1.73, 1.46	1.46	0.87
Phe2		5.09	3.17	3.07	
Ala3	8.21	4.54	1.21		
Pro4		4.3	1.98, 1.85	1.85, 1.78	3.48
Leu5	7.87	4.13	1.54, 1.41	1.41	0.86, 0.82
	11: Fmoc–Leu–Ψ[CON(OBz)]–Phe–Ala–OBu^t				
	NH	Hα	Hβ	Hγ	Hδ
Leu	5.34	4.86	1.67, 1.39	1.21	0.89, 0.81
Phe		4.96	3.60, 3.52		
Ala	7.09	4.49	1.41		
	12: Fmoc–Leu–Ψ[CON(OBz)]–Phe–Ala–Pro–OBu^t				
	NH	Hα	Hβ	Hγ	Hδ
Leu	5.37	4.86	1.63, 1.39	1.39	0.85, 0.74
Phe		4.98	3.51, 3.39		
Ala	7.1	4.71	1.34		
Pro		4.4	2.17, 2.03	1.96	3.65, 3.56
	18: Fmoc–[Leu–Ψ[CON(OBz)]–Phe–$Ala]_2$–OBu^t				
	NH	Hα	Hβ	Hγ	Hδ
Leu1	5.35	4.75	1.60, 1.35	1.16	0.83, 0.74
Phe2		4.8	3.54, 3.44		
Ala3	7.06	4.41	1.35		
Leu4	6.61	4.92	1.48, 1.34	1.11	0.74, 0.64
Phe5		4.77	3.48, 3.39		
Ala6	7.02	4.41	1.34		
	15: Fmoc–[Leu–Ψ[CON(OBz)]–Phe–Ala–$Pro]_2$–OBu^t				
	NH	Hα	Hβ	Hγ	Hδ
Leu1	5.53	4.78	1.62, 1.38	1.25	0.82, 0.73
Phe2		4.93	3.50, 3.41		
Ala3	7.19	4.66	1.36		

Table III (*Continued*)

	15: Fmoc–[Leu–Ψ[CON(OBz)]–Phe–Ala–Pro]$_2$–OBu^t				
	NH	Hα	Hβ	Hγ	Hδ
Pro4		4.51	2.25, 2.07	1.94, 1.79	3.60, 3.50
Leu5	6.98	4.84	1.45, 1.30	1.16	0.74, 0.63
Phe6		4.79	3.48, 3.37		
Ala7	7.17	4.68	1.3		
Pro8		4.43	2.13, 2.00	1.94	3.67, 3.56
	21: Fmoc–Val–Ψ[CON(OBz)]–Phe–Ala–Leu–NHOBz				
	NH	Hα	Hβ	Hγ	Hδ
Val	5.49	4.62	1.94	0.85	
Phe		4.7	3.50, 3.38		
Ala	6.8	4.19	1.32	0.88	
Leu	6.74	4.24	1.75, 1.56	1.51	0.86

flash chromatography with silica gel. The semi-preparative HPLC and analytical HPLC analyses were performed on Vydac C-18 columns using a linear gradient of 0.1% TFA in H_2O and 0.1% TFA in CH_3CN flow rate (detection at 214 nm, analysis at 1.0 mL/min, and purification at 9.5 mL/min). All the solvents including DMF, acetonitrile, dichloromethane (DCM), methanol, hexane, toluene, and ethyl acetate were obtained from Fisher Scientific. HBTU, DIEA, piperidine, and all Fmoc–amino acids were ordered from Advanced ChemTech (Louisville, KY); All metal salts [nickel(II) chloride hexahydrate 99.999%, zinc sulfate heptahydrate 99.999%, iron(III) nitrate nonahydrate 99.99%, copper(II) sulfate pentahydrate 99.999%, iron(II) sulfate hepahydrate 99.99%, cobalt(II) nitrate heptahydrate, manganese(II) chloride, gallium(III) sulfate 99.999%], and other chemicals were purchased from Aldrich Chemical Co.

N-Benzyloxy-Glycine *tert*-Butyl Ester (1)

To a solution of $BzONH_2$ (2.71 g, 22.0 mmol) and DIEA (1.55 g, 12.0 mmol) in THF (20 mL) was added dropwise *tert*-butyl bromoacetate (2.15 g, 11.0 mmol) in THF (15 mL). The resulting solution was refluxed under nitrogen atmosphere for 8 h. After the solvent was removed under reduced pressure, the residual oil was dissolved in CH_2Cl_2 (20 mL); successively washed with H_2O, 5% aqueous citric acid, 5% aqueous $NaHCO_3$, and brine; dried over Na_2SO_4; and filtered. Evaporation of the solvent under reduced pressure gave a crude product, which was then purified by flash chromatography on silica gel using hexane/CH_2Cl_2 (100:0, 100:20, 100:40, 60:40) as eluent to afford 2.22 g (65 % yield) of **1** as an oil.

N-Benzyloxy-Alanine *tert*-Butyl Ester (2)

To a stirred and cooled (−15°C) solution of *tert*-butyl (R)-(+) lactate (2.0 g, 13.68 mmol) in CH_2Cl_2 (15 mL), was added dropwise a solution of trifluoromethanesulfonic anhydride (4.63 g, 16.41 mmol) in CH_2Cl_2 (10 mL), following by adding 2,6-lutidine (1.80 g, 16.80 mmol). After 30 min, *O*-benzyl-hydroxyamine (2.5 g, 20.3 mmol) was added and the reaction mixture was stirred at 0°C for 30 min and room temperature for 2 h. The solvent was removed, and the residue was dissolved in CH_2Cl_2; washed with H_2O, 5% aqueous citric acid, 5% aqueous $NaHCO_3$, and brine; dried over Na_2SO_4; and filtered. Evaporation of the solvent under reduced pressure gave a crude product, which was then purified by flash chromatography on silica gel using hexane/CH_2Cl_2 (100:0, 100:20, 80:20) as the eluent to afford the title compound **2** as an oil (1.8 g, 53%).

D-3-Phenyllactic Acid Allyl Ester (4)

To a stirred solution of D-3-phenyllactic acid (3.50 g, 21.06 mmol) in 5% $NaHCO_3$ (36 mL) was added allyl bromide (2.80 g, 23.14 mmol) and Aliquat 336 (8.51 g, 21.06 mmol) in CH_2Cl_2 (40 mL). The reaction mixture was stirred vigorously for 120 h. The organic layer was separated and the aqueous layer was extracted with CH_2Cl_2 (2 × 10 mL). The combined CH_2Cl_2 was dried over anhydrous K_2CO^3, concentrated, and purified by flash column chromatrography (CH_2Cl_2/hexane, 100:0, 100:20, 100:40, 50/50) to afford the title compound **4** as a colorless oil (3.9 g, 89% yield).

N-Benzyloxy-Phenylalanine Allyl Ester (5)

The title compound was prepared from **4** (3.0 g, 14.55 mmol) under the same conditions described for **2.** The crude product was purified by flash column chromatography on silica gel using CH_2Cl_2/hexane (100:0, 100:40, 100:60, 40:60) as the eluent to afford **5** (2.50 g, 55% yield).

N-Benzyloxy-Phenylalanine (3)

To a mixture of **5** (2.0 g, 6.42 mmol) and tetrakis(triphenylphosphine) palladium(0) (0.74 g, 0.64 mmol) in THF (10 mL) under a nitrogen atmosphere was added morpholine (6.6 g, 75.75 mmol). The reaction mixture was stirred at room temperature for 2 h. The solvent was removed under reduced pressure and the residue was dissolved in 5% $NaHCO_3$ and filtered; the filtrate was acidified with 1N HCl. The precipitate was collected by filtration and dried to afford **3** (1.5 g, 86% yield). This crude product was used without further purification. Fifty milligrams of the crude product was further purified using HPLC to give 38.2 mg of pure **3.** ES-MS: Observed for $[MH]^+$: *m/z* 272.15.

Fmoc–Val–Ψ[CON(OBz)]Gly–OBu^t (6a)

To a stirred solution of **1** (1.0 g, 4.21 mmol) and Fmoc–Val–Cl (1.80 g, 5.03 mmol) in 15 mL of toluene was added AgCN (0.70 g, 5.23 mmol). The mixture was stirred at room temperature for 8 h. The insoluble material was filtered off, and the solvent was removed under reduced pressure. The residue was taken up in CH_2Cl_2 and purified by flash column chromatography on silica gel (CH_2Cl_2/CH_3OH, 100:0, 100:0.5, 99:1) to afford **6a** (1.75 g, 75%). ES-MS: Observed for $[MH]^+$: *m/z* 559.31.

Fmoc–Val–Ψ[CON(OBz)]–Ala–OBu^t (6b)

Using the same procedure as described for **6a,** the title compound was prepared from **2** (1:0 g, 3.98 mmol) and Fmoc–Val–Cl (1.44 g, 4.02 mmol) and AgCN (0.66 g, 4.94 mmol). Purification by flash column chromatrography using CH_2Cl_2/CH_3OH (100:0, 100: 0.5, 100:1) as the eluent afforded 1.64 g (72%) of **6b** as a white solid. ES-MS: Observed for $[MH]^+$: *m/z* 573.27.

Ψ(OBz)–Phe–Ala–OBu^t (10)

To a stirred and cooled solution of **3** (1.0 g, 3.69 mmol), HOBT (0.50 g, 3.69 mmol), H–Ala–OBu^t-HCl (0.81 g, 4.46 mmol), and *N*-ethylmorpholine (0.51 g, 4.43 mmol) in DMF (15 mL) was added EDCI (0.88 g, 4.59 mmol). The reaction mixture was stirred at room temperature for overnight. After the solvent was removed under reduced pressure, the residue was dissolved in CH_2Cl_2 (25 mL), successively washed with H_2O, 5% aqueous citric acid, and 5% aqueous $NaHCO_3$, and brine, dried over Na_2SO_4, and filtered. Evaporation of the solvent under reduced pressure gave a crude product that was purified by flash chromatography on silica gel using CH_2Cl_2/CH_3OH (100:0, 100:0.5) as the eluent to afford 1.21 g (82%) of **10** as a white solid.

Fmoc–Leu–Ψ[CON(OBz)]–Phe–Ala–OBu^t (11)

The title compound was prepared from **10** (2.0 g, 5.02 mmol), Fmoc–Leu–Cl (2.24 g, 6.02 mmol), and AgCN (0.82 g, 6.12 mmol) using the same procedure described for **6.** Purification by flash column chromatography using CH_2Cl_2/CH_3OH (100:0, 100:0.5, 100:1) as the eluent afforded 3.1g (84%) of **11** as a white solid. ES-MS: Observed for $[MH]^+$: *m/z* 734.39.

Fmoc–Leu–Ψ[CON(OBz)]–Phe–Ala–Pro–OBu^t (12)

Compound **11** (2.0 g, 2.73 mmol) was dissolved in TFA (15 mL), stirred for 20 min, concentrated, and dried under vacuum overnight. The obtained acid was dissolved in DMF (15 mL) together with Pro–OBu^t (0.56 g, 3.29 mmol) and HOBT (0.44 g, 3.25 mmol). To this stirred and cooled (0°C) solution, EDCI (0.63 g, 3.29 mmol) was added. The reaction mixture was stirred at room temperature, concentrated under vacuum and dissolved in CH_2Cl_2 (30 mL). The solution was washed successively with H_2O, 5% aqueous citric acid, 5% aqueous $NaHCO_3$, and brine; dried over Na_2SO_4; and filtered. Evaporation of the solvent gave a crude product that was purified by flash chromatography on silica gel using CH_2Cl_2/CH_3OH (100:0, 100:0.5, 100:1, 100:2) as the eluent to afford 1.58 g (70%) of **12** as a white solid. ES-MS: Observed for $[MH]^+$: *m/z* 831.45.

Fmoc–{Leu–Ψ[CON(OBz)]–Phe–Ala–Pro}$_2$–OBu^t (15)

Compound **12** (0.5 g, 0.60 mmol) was dissolved in TFA (8 mL), stirred for 20 min, concentrated, and dried under vacuum to afford the acid intermediate **13.** Compound **12** (0.5 g, 0.60 mmol) was dissolved in 20% piperidine/DMF (10 mL) solution, stirred for 15

min, concentrated under vacuum, treated with hexane (3 × 5 mL). The unsoluble residue was dried under vacuum to afford the amine intermediate **14.** To a stirred solution of **13** and **14,** HOBT (0.10 g, 0.74 mmol), and PyBOP (0.38 g, 0.73 mmol) in DMF (10 mL) at room temperature was added DIEA (0.19 g, 1.47 mmol). The reaction mixture was stirred for 8 h and concentrated under vacuum. The residue was dissolved in CH_2Cl_2; successively washed with H_2O, 5% aqueous citric acid, 5% aqueous $NaHCO_3$; and brine, dried over Na_2SO_4; and filtered. The solvent was removed under reduced pressure to give a crude product that was purified by flash chromatography on silica gel using CH_2Cl_2/CH_3OH (100:0, 100:0.5, 100:1, 100:1.5, 100:2, 100:2.5) as the eluent to afford 0.45 g (55%) of **15** as a white solid. ES-MS: Observed for $[MH]^+$: *m/z* 1365.63.

Cyclo{Leu–Ψ[CON(OBz)]–Phe–Ala–Pro}$_2$ (17)

Compound **15** (0.20 g, 0.15 mmol) was dissolved in TFA (5 mL), stirred for 20 min at room temperature, concentrated, and dried under vacuum. This obtained acid intermediate was dissolved in 20% piperidine/DMF (5 mL), stirred for 15 min, concentrated, and treated with hexane (3 × 5 mL). The unsoluble residue was dissolved in DMF (800 mL). To this stirred solution were added DIEA (38.8 mg, 0.30 mmol), HOBT (20.3 mg, 0.15 mmol), and PyBOP (106.1 mg, 0.20 mmol). The reaction mixture was stirred at room temperature for 72 h, and concentrated. The residue was dissolved in CH_2Cl_2 (20 mL); successively washed with H_2O, 5% aqueous citric acid, 5% aqueous $NaHCO_3$, and brine; dried over Na_2SO_4; and filtered. Evaporation of the solvent under reduced pressure gave a crude product that was purified by flash chromatography on silica gel using CH_2Cl_2/CH_3OH (100:0, 100:0.5, 100:1, 100:1.5, 100:2, 100:2.5) as the eluent to afford 96.2 mg (60%) of **17** as a white solid. ES-MS: Observed for $[MH]^+$: *m/z* 1069.00.

Cyclo{Leu–Ψ[CON(OH)]–Phe–Ala–Pro}$_2$ (P8)

Compound **17** (95 mg, 0.089 mmol) was dissolved in cooled CH_3OH (10 mL). To this stirred solution was added 5% Pd/C (35 mg), followed by ammonium formate (100 mg, 1.59 mmol). The mixture was stirred at room temperature for 4 h, filtered, concentrated, and purified by preparative HPLC (CH_3CN/H_2O gradient, 5–80%, 30 min). The pure fractions were identified by ESI-MS, combined, and lyophilized to afford **P8** (29.3 mg, 37%) as a white solid. ES-MS: Observed for $[MH]^+$: *m/z* 889.70.

H–{Leu–Ψ[CON(OH)]–Phe–Ala–Pro}$_2$–OH• TFA (P7)

Compound **15** (100 mg, 0.073 mmol) was similarly deblocked first with TFA and then 20% piperidine as described for **17.** The obtained crude material was dissolved in cooled CH_3OH (10 mL). To this stirred solution was added 5% Pd/C (35 mg), followed by ammonium formate (100 mg, 1.59 mmol). The mixture was stirred at room temperature for 4 h, filtered, concentrated, and purified by preparative HPLC (CH_3CN/H_2O gradient, 5–80%; 30 min) to afford **P7** (23.1 mg, 31%) as a white solid. ES-MS: Observed for $[MH]^+$: *m/z* 907.71.

Fmoc–{Leu–Ψ[CON(OBz)]–Phe–Ala}$_2$–OBu^t (18)

The title compound was similarly prepared from **11** (0.44 g, 0.60 mmol) as described for **15.** The crude product was purified by flash chromatography on silica gel using CH_2Cl_2/CH_3OH (100:0, 100:0.5, 100:1, 100:1.5, 100:2) as the eluent to afford 0.32 g (46%) of the desired product as a white solid. ES-MS: Observed for $[MH]^+$: *m/z* 1171.63.

Cyclo{Leu–Ψ[CON(OBz)]–Phe–Ala}$_2$ (19)

The title compound was prepared from **18** (0.20 g, 0.17 mmol) using the same procedure described for **17.** Purification by flash chromatography on silica gel using CH_2Cl_2/CH_3OH (100:0, 100:0.5, 100:1, 100:1.5, 100:2) as the eluent gave 70.0 mg (47%) of **19** as a white solid. ES-MS: Observed for $[MH]^+$: *m/z* 875.76.

H–{Leu–Ψ[CON(OH)]–Phe–Ala}$_2$–OH (P5)

Using the same procedure as described for **P7,** the title compound (18.3 mg, 26%) was prepared from **18** (100.0 mg, 0.085 mmol). ES-MS: Observed for $[MH]^+$: *m/z* 713.56.

Cyclo{Leu–Ψ[CON(OH)]–Phe–Ala}$_2$ (P6)

The title compound was prepared from **19** (70.0 mg, 0.08 mmol) using the same procedure as described for **P8** (15.0 mg, 27%). ES-MS: Observed for $[MH]^+$: *m/z* 695.43.

Fmoc–Val–Ψ[CON(OBz)]–Phe–Ala–OBu^t (20)

The title compound was prepared from **10** (1.0 g, 2.51 mmol), Fmoc–Val–Cl (1.08 g, 3.02 mmol), and AgCN (0.41 g, 3.06 mmol) using the same procedure as described for **6a.** Purification by flash column chromatography on silica gel using CH_2Cl_2/CH_3OH (100:0, 100:0.5, 100:1) as the eluent afforded 1.43 g (79%) of **20** as a white solid.

Fmoc–Val–Ψ[CON(OBz)]–Phe–Ala–Leu–NHOBz (21)

Compound **20** (1.0 g, 1.39 mmol) was dissolved in TFA (10 mL), stirred for 20 min, concentrated, and dried under vacuum. The obtained acid intermediate was dissolved in DMF (15 mL) together with H–Leu–NHOBz (0.394 g, 1.67 mmol) and HOBT (0.23 g, 1.70 mmol), and dissolved. To this stirred solution at 0°C was added EDCI (0.33 g, 1.72 mmol). The reaction mixture was stirred for 4 h. The solvent was removed under vacuum, and the residue was dissolved in CH_2Cl_2 (20 mL); successively washed with H_2O, 5% aqueous citric acid, 5% aqueous $NaHCO_3$, and brine; dried over Na_2SO_4; and filtered. Evaporation of the solvent under reduced pressure gave a crude product that was then purified by flash chromatography on silica gel using CH_2Cl_2/CH_3OH (100:0, 100:0.5, 100:1) as the eluent to afford 0.74 g (60%) of **10** as a white solid. ES-MS: Observed for $[MH]^+$: *m/z* 883.48.

H–Val–Ψ[CON(OH)]–Phe–Ala–Leu–NHOH (P3)

Compound **21** (0.5 g, 0.57 mmol) was dissolved in 20% piperidine/DMF (10 mL), stirred for 15 min, concentrated, and treated with hexane (3 × 10 mL). The insoluble residue was dissolved in CH_3OH (20 mL). To this stirred solution was added 5% Pd/C (100 mg), followed by ammonium formate (300 mg, 4.76 mmol). The mixture was stirred at room temperature for 4 h, filtered, concentrated, and purified by preparative HPLC (CH_3CN/H_2O gradient, 5–60%, 30 min). The pure fractions were identified by ESI-MS, combined, and lyophilized to afford **P3** (0.14 g, 41%). ES-MS: Observed for $[MH]^+$: *m/z* 480.64.

H–Leu–Ψ[CON(OH)]–Phe–Ala–Pro–Leu–NHOH (P9)

The title compound was prepared from **12** (500 mg, 0.60 mmol) via Fmoc–Leu–Ψ[CON(OBz)]–Phe–Ala–Pro–Leu–NHOBz using the similar procedure as described for **P3.** Purification by HPLC afforded 127.0 mg in an overall yield of 30%. ES-MS: Observed for $[MH]^+$: *m/z* 591.47.

Synthesis of H–Leu–Ψ[CON(OH)]–Ala–Ala–Pro–Leu–NHOH (P10) on a Solid Support

The peptide was prepared manually on *N*-Fmoc-hydroxylamine 2-chlorotrityl resin (0.7 mmol/g, 1 g). The resin was preswollen in DCM for 1 h and then deblocked with 20% piperidine in DCM for 20 min. After washing with DCM (5 × 2 mL) and DMF (5 mL × 3), the first residue Fmoc–Leu was attached by reacting the resin with a solution of Fmoc–Leu (5 equiv), HATU (4 equiv); and DIPEA (4 equiv) of in DMF for 18 h. The chain elongation was realized using a conventional Fmoc–AA/HBTU/HOBT/DIEA coupling protocol. Ψ[N(OH)]–Ala was incorporated into resin-bound peptide by using a mixture of Ψ[N(OH)]–Ala (3 equiv)/DIC (3 equiv)/HOBT (3 equiv) for 16 h. After it was filtered and washed with DMF (5 mL × 3), the resulting resin-bound peptide was reacted with a solution of Fmoc–Leu (3 equiv)/HATU (2 equiv)/DIEA (2 equiv) in DMF for another 16 h. It was filtered, washed with DMF, and deblocked with 20% piperidine/DMF for 20 min. The resin was treated with TFA:water:triisopropylsilane (95:2.5:2.5) (0.5 h × 3) to provide the crude product (130 mg), that was deblocked similarly using ammonium formate in the presence of Pd/C(5%) in methanol as described for compound **P10.** The crude peptide hydroxylamide was purified by semipreparative HPLC to afford the desired compound (57 mg, 13%). ES-MS: Observed for $[MH]^+$: *m/z* 515.33.

Preparation of Test Solutions of Metal Complex for ESI-MS, HPLC, and UV-Vis Analysis

Stock solutions (1 m*M*) of the peptide ligands and some metal salts including $CuSO_4 \cdot 5H_2O$, $MnCl_2$, $ZnSO_4 \cdot 7H_2O$, $NiCl_2 \cdot 6H_2O$, $Co(NO_3)_2 \cdot 6H_2O$, $FeSO_4 \cdot 7H_2O$, $CdCl_2$, and $Fe(NO_3)_3) \cdot 9H_2O$, $Ga_2(SO_4)_3$ in methanol or water were first prepared. Typically, test solutions (300 μL each) containing 100 μ*M* of ligands were then prepared by mixing 30 μL of a ligand stock solution and 30 μL of a metal stock solution in 240 μL of methanol. Different aliquots of a metal solution were added to afford test solutions with different metal/ligand ratios for titration studies while different metal solutions were added into one solution for competition experiments. All the test solutions were shaken for 8 h to insure equilibrium before subjecting to ESI-MS analysis.

Preparation of 20@Ga^{3+} Complex for 2D ^{1}H-NMR Studies

The amount of 3.8 mg of $Ga_2(SO_4)_3$ and 4.0 mg of **20** (i.e., **8** in Table I) were first dissolved in 7 mL of CH_3CN/H_2O (7:3). The resulting solution was stirred at room temperature overnight and lyophilized to afford a dry white solid that was dissolved in d_6-DMSO and filtered for ^{1}H-NMR experiments.

^{1}H-NMR Experiments

NMR spectra were recorded with a Varian Inova-600 (Varian Inc., Palo Alto, CA) spectrometer and the data were processed with VNMR software. The TOCSY spectra were recorded using a MELV-17 mixing sequence of 120 ms flanked by two 2 ms trim pulses. Phase-sensitive 2D, spectra were obtained by employing the hypercomplex method. A total of 2 $\times$ 256 $\times$ 2048 data matrix with 16 scans per t1 increment were collected. Gaussian and sine-bell apodization functions were used in weighting the t2 and t1 dimensions, respectively. After two-dimensional Fourier transformation, the 2048 $\times$ 2048 frequency domain representation was phase and baseline corrected in both dimensions. The NOESY spectrum resulted in a 2 $\times$ 256 $\times$ 2049 data matrix with 32 scans per t1 increment. Spectra were recorded with 250 and 420 ms mixing time. The use of a 420 ms mixing time (at 298 K) afforded a better result. The hypercomplex method was used to yield phase-sensitive spectra. The time domain data were zero filled to yield a 2048 $\times$ 2048 data matrix and were processed in a similar way as the 2D TOCSY spectrum described above.

We acknowledge the National Institutes of Health (GM 53630) for partial support of this research. The Washington University Mass Spectroscopy Resource Center partially supported by NIH (RR00954) and the Washington University High Resolution NMR Resource Center (NIH RR02004, RR05018, and RR07155) were utilized to characterize the peptide analogs synthesized as part of this study.

REFERENCES

1. Orvig, C.; Abrams, M. J. Chem Rev 1999, 99, 2201–2842.
2. Laity, J. H.; Lee, B. M.; Wright, P. E. Curr Opin Struct Biol 2001, 11, 39–46.
3. Marshall, G. R.; Reddy, P. A.; Schall, O. F.; Naik, A.; Beusen, D. B.; Ye, Y.; Slomczynska, U. In Advances in Supermolecular Chemistry; Gokel, G. W., Ed.; Cerebus Press: Miami, FL, 2002; Vol 8.
4. Ye, Y.; Marshall, G. R. In Peptides: The Wave of the Future (Proceedings of the 17th American Peptide Symposium); Lebl, M., Houghten, R. A., Eds.; American Peptide Symposium: San Diego, CA, 2001, pp. 591–592.
5. Ye, Y.; Marshall, G. R. In Peptides: The Wave of the Future (Proceedings of the 17th American Peptide Symposium); Lebl, M., Houghten, R. A., Eds.; American Peptide Society: San Diego, CA, 2001, pp. 589–590.
6. Ye, Y.; Marshall, G. R. In Peptides: The Wave of the Future (Proceedings of the 17th American Peptide Symposium); Lebl, M., Houghten, R. A., Eds.; American Peptide Society: San Diego, CA, 2001, pp. 595–596.
7. Ye, Y.; Marshall, G. R.; Smith, R.; Darmstoff, C.; Slomczynska, U. In Peptides: The Wave of the Future (Proceedings of the 17th American Peptide Symposium); Lebl, M., Houghten, R. A., Eds.; American Peptide Society: San Diego, CA, 2001, pp. 593–594.
8. Tian, Z.-Q.; Bartlett, P. A. J Am Chem Soc 1996, 118, 943–949.
9. Sharma, S. D. U.S. Patent #5,891,418, April 6, 1999, Rhomed, Inc. Albuquerque, NM
10. Shi, Y.; Cai, H.-Z.; Yang, W. H.; Blood, C.; Shadiack, A.; Sharma, S. Abstracts of the 218th ACS National Meeting, New Orleans, LA, 1999; p MEDI-257.
11. Shi, Y.; Sharma, S. Bioorg Med Chem Lett 1999, 9, 1469–1474.
12. Giblin, M. F.; Wang, N.; Hoffman, T. J.; Jurisson, S. S.; Quinn, T. P. Proc Natl Acad Sci USA 1998, 95, 12814–12818.
13. Ruan, F.; Chen, Y.; Hopkins, P. B. J Am Chem Soc 1990, 112, 9403–9404.
14. Ghadiri, M. R.; Choi, C. J Am Chem Soc 1990, 112, 1630–1632.
15. Ghadiri, M. R.; Fernholz, A. K. J Am Chem Soc 1990, 112, 9633–9635.
16. Imperiali, B.; Kapoor, T. M. Tetrahedron 1993, 49, 3501–3510.
17. Schneider, J. P.; Kelly, J. W. J Am Chem Soc 1995, 117, 2533–2546.
18. Cheng, R. P.; Fisher, S. L.; Imperiali, B. J Am Chem Soc 1996, 118, 11349–11356.
19. Kohn, W. D.; Kay, C. M.; Sykes, B. D.; Hodges, R. S. J Am Chem Soc 1998, 120, 1124–1132.
20. Suzuki, K.; Hiroaki, H.; Kohda, D.; Nakamura, H.; Tanaka, T. J Am Chem Soc 1998, 120, 13008–13015.
21. Schwartz, T. W.; Hjorth, S. A.; Kastrup, J. S., Eds. Structure and Function of 7TM Receptors; Munksgaard: Copenhagen, 1996; Vol 39.
22. Sheikh, S. P.; Zvyaga, T. A.; Lichtarge, O.; Sakmar, T. P.; Bourne, H. R. Nature 1996, 383, 347–350.
23. Reaka, A. J. H.; Ho, C. M. W.; Marshall, G. R. J Comput-Aid Mol Des 2003, 16, 585–600.
24. Bunin, B. A.; Ellman, J. A. J Am Chem Soc 1992, 114, 10997–10998.
25. Ostresh, J. M.; Husar, G. M.; Blondelle, S. E.; Dorner, B.; Weber, P. A.; Houghten, R. A. Proc Natl Acad Sci USA 1994, 91, 11138–11142.

26. Nefzi, A.; Ostresh, J. M.; Houghten, R. A. Biopolymers 2001, 60, 212–219.
27. Huang, L.; Lee, A.; Ellman, J. A. J Med Chem 2002, 45, 676–684.
28. Blaney, P.; Grigg, R.; Sridharan, V. Chem Rev 2002, 102, 2607–2624.
29. Krchnak, V.; Holladay, M. W. Chem Rev 2002, 102, 61–91.
30. Winkelmann, G. In CRC Handbook of Microbial Iron Chelates; Winkelmann, G., Ed.; CRC Press: Tubingen, 1991.
31. Nishino, N.; Powers, J. C. Biochemistry 1978, 17, 2846–2850.
32. Nishino, N.; Powers, J. C. Biochemistry 1979, 18, 4340–4347.
33. Bourdel, E.; Doulut, S.; Jarretou, G.; Labbe-Jullie, C.; Fehrentz, J. A.; Doumbia, O.; Kitabgi, P.; Martinez, J. Int J Pept Protein Res 1996, 48, 148–155.
34. Patel, D. V.; Young, M. G.; Robinson, S. P.; Hunihan, L.; Dean, B. J.; Gordon, E. M. J Med Chem 1996, 39, 4197–4210.
35. Fray, M. J.; Dickinson, R. P. Bioorg Med Chem Lett 2001, 11, 571–574.
36. Hanessian, S.; Moitessier, N.; Gauchet, C.; Viau, M. J Med Chem 2001, 44, 3066–3073.
37. Nar, H.; Werle, K.; Bauer, M. M.; Dollinger, H.; Jung, B. J Mol Biol 2001, 312, 743–751.
38. Hin, S.; Zabel, C.; Bianco, A.; Jung, G.; Walden, P. J Immunol 1999, 163, 2363–2367.
39. Bianco, A.; Zabel, C.; Walden, P.; Jung, G. J Pept Sci 1998, 4, 471–478.
40. Marastoni, M.; Bazzaro, M.; Salvadori, S.; Bortolotti, F.; Tomatis, R. Bioorg Med Chem 2001, 9, 939–945.
41. Akiyama, M.; Katoh, A.; Mutsui, Y.; Watanabe, Y.; Umemoto, K. Chem Lett 1996, 915–916.
42. Hara, Y.; Akiyama, M. Inorg Chem 1996, 35, 5173–5180.
43. Hara, Y.; Shen, L.; Tsubouchi, A.; Akiyama, M.; Umemoto, K. Inorg Chem 2000, 39, 5074–5082.
44. Hara, Y.; Akiyama, M. J Am Chem Soc 2001, 123, 7247–7256.
45. Caudle, M. T.; Stevens, R. D.; Crumbliss, A. L. Inorg Chem 1994, 33, 843–844.
46. Muller, G.; Isowa, Y.; Raymond, K. J Biol Chem 1985, 260, 13921–13926.
47. Muller, G.; Barelay, S.; Raymond, K. J Biol Chem 1985, 260, 13916–13920.
48. Herscheid, J. D. M.; Colstee, J. H.; Ottenheijm, H. C. J. J Org Chem 1981, 46, 3346–3348.
49. Chen, J. J.; Spatola, A. F. Tetrahedron Lett 1997, 38, 1511–1514.
50. Mellor, S. L.; McGuire, C.; Chan, W. C. Tetrahedron Lett 1997, 38, 3311–3314.
51. Wang, L.; Phanstiel IV, O. J Org Chem 2000, 65, 1442–1447.
52. Olsen, R. K.; Ramasamy, K. J Org Chem 1985, 50, 2264–2271.
53. Akiyama, M.; Iesaki, K.; Katoh, A.; Shimizu, K. J Chem Soc Perkin I 1986, 851–855.
54. Akiyama, M.; Ikeda, T. Chem Lett 1995, 849–850.
55. Ottenheijm, H. C. J.; Herscheid, J. D. M. Chem Rev 1986, 86, 697–707.
56. Feenstra, R. W.; Stokkingreef, E. H. M.; NIvard, R. J. F.; Ottenheijm, H. C. J. Tetrahedron Lett 1987, 28, 1215–1218.
57. Fields, J. D.; Kropp, P. J. J Org Chem 2000, 65, 5937–5941.
58. Wittman, M. D.; Halcomb, R. L.; Danishefsky, S. J. J Org Chem 1990, 55, 1981–1983.
59. Murray, R. W.; Singh, M. Synth Commun 1989, 19, 3509–3522.
60. Tokuyama, H.; Kuboyama, T.; Amanao, A.; Yamashita, T.; Fukuyama, T. Synthesis 2000, 1299–1304.
61. Grundke, G.; Keese, W.; Rimple, M. Synthesis 1987, 1115–1116.
62. Lin, Y.-M.; Miller, M. J. J Org Chem 1999, 64, 7451–7458.
63. Polonski, T.; Chimiak, A. Tetrahedron Lett 1974, 28, 2453–2456.
64. Friedrich-Bochnitschek, S.; Waldmann, H.; Kuntz, H. J Org Chem 1989, 54, 751–756.
65. Albericio, F.; Carpino, L. A. Methods Enzymol 1997, 289, 104–126.
66. Perlow, D. S.; Erb, J. M.; Gould, N. P.; et al. J Org Chem 1992, 57, 4394–4400.
67. Braslau, R.; Axon, J. R.; Lee, B. Org Lett 2000, 2, 1399–1401.
68. Coste, J.; Le-Nguyen, D.; Castro, B. Tetrahedron Lett 1990, 31, 205–208.
69. Kaiser, E.; Colescott, R. L.; Bossinger, C. D.; Cook, P. I. Anal Biochem 1970, 34, 595–598.
70. Carpino, L. A. J Am Chem Soc 1993, 115, 4397–4398.
71. Reddy, P. A.; Schall, O. F.; Wheatley, J. R.; Rosik, L. O.; McClurg, J. P.; Marshall, G. R.; Slomezynska, U. Synthesis—Stuttgart 2001, 1086–1092.
72. Slomezynska, U.; Reddy, P. A.; Schall, O. F.; Osrek, T.; Nauk, A.; Edwards, W. B.; Wheatley, J.; Marshall, G. R. In Peptides: The Wave of the Future (Proc. 17th American Peptide Symp.); Lebl, M., Houghten, R. A., Eds.; American Peptide Society: San Diego, CA, 2001.
73. Schalley, C. A.; Castellano, R. K.; Brody, M. S.; Rudkevich, D. M.; Siuzdak, G.; Julius Rebek, J. J Am Chem Soc 1999, 4568–4579.
74. Schalley, C. A.; Castellano, R. K.; Brody, M. S.; Rudkevich, D. M.; Siuzdak, G.; Julius Rebek, J. J Am Chem Soc 1999, 121, 4568–4579.
75. Manna, J.; Kuehl, C. J.; Whiteford, J. A.; Stang, P. J.; Muddiman, D. C.; Hofstadler, S. A.; Smith, R. D. J Am Chem Soc 1997, 119.
76. Leong, J.; Raymond, K. N. J Am Chem Soc 1975, 97, 293–296.
77. Pearson, R. G. J Am Chem Soc 1963, 85, 3533–3539.
78. Parr, R. G.; Pearson, R. G. J Am Chem Soc 1983, 105, 7512–7516.
79. Martell, A. E.; Hancock, R. D. Metal Complexes in Aqueous Solution; Plenum Press: New York, 1996.
80. Albericio, F.; Carpino, L. A. Methods Enzymol 1997, 289, 104–126.
81. Bergeron, R. J.; McManis, J. S.; Phanstiel IV, O.; Vinson, J. R. J Org Chem 1995, 60, 109–114.